Tongxiao Zhang
College of Information and
Electrical Engineering,
China University of Mining and Technology,
Jiangsu, Xuzhou 221116, China
e-mail: cheshenztx@126.com

Mamoru Minami
Graduate School of Natural
Science and Technology,
Okayama University 3-1-1 Tsushimanaka,
Okayama 7008530, Japan
e-mail: minami@sys.okayama-u.ac.jp

Osami Yasukura
Graduate School of Engineering,
University of Fukui,
Fukui 9108507, Japan
e-mail: yasukura@apphy.u-fukui.ac.jp

Wei Song
School of Mechatronics
Engineering and Automation,
Shanghai University,
149 Yanchang Road,
Shanghai 200072, China
e-mail: song_wei@shu.edu.cn

Reconfiguration Manipulability Analyses for Redundant Robots

This paper is concerned with a concept of reconfiguration manipulability inspired from manipulability. The reconfiguration manipulability represents a shape-changeability of each intermediate link when a prior end-effector task is given. Through analyses of reconfiguration matrices, we propose a method to judge whether the plural shape-changing subtasks can be executed simultaneously or not. Then the sufficient conditions guaranteeing sustainability of reconfiguration manipulability space are presented, which are the conditions for keeping the reconfiguration manipulability as high as possible under the prior end-effector task. Further, we confirm the proposed analyses can be useful practically for evaluating the realistic manipulator's configurations and structures.
[DOI: 10.1115/1.4024727]

1 Introduction

KINEMATICALLY redundant manipulators have more DoF than necessary for accomplishing a given end-effector task. Nowadays, redundant manipulators are used for various kinds of tasks such as welding, sealing, grinding, and contact tasks. Many kinematic researches have used the redundancy to solve the problem of motion and obstacle avoidance. Up to now, a variety of indices have been proposed for evaluation of the performance of robot manipulators. The manipulability [1,2] was presented to indicate the manipulator's ability on the view point of how much the velocity of each link can be generated by normalized joint velocity as the static performance of the manipulator. Further, Ref. [3] formulated the relation of the redundancy and the priority order of multiple tasks. Reference [4] proposed a control method of the redundancy based on priority order of tasks, and pointed out the effectiveness by actual experiments. The manipulability concept was used for cooperative arms [5–7] and for dexterous hands [8] and was used in real-time control [9]. In Ref. [7], the authors propose a novel method for a finger-arm robot to complete an impedance control by regulating fingers manipulability in a constrained task. In Ref. [9], a real-time control strategy to optimize control performance index by using the conjugate gradient method is presented. But the realizability of reconfiguration subtasks of the intermediate links is not discussed. In addition, the manipulating force ellipsoid [10] was presented to evaluate the static torque-force transmission from the joints to the end-effector, while the dynamic manipulability ellipsoid [11] was presented as an index of the dynamic performance of a robot manipulator. In Ref. [12], a new definition of a dynamic manipulability ellipsoid for redundant manipulators is proposed which leads to more correct results in evaluating manipulator capabilities in terms of task-space

accelerations. The concept of inertia matching for a serial-link manipulator [13] was recently proposed as a new index of the dynamic performance of a manipulator. Then, combining the dynamic manipulability ellipsoid with the manipulability force ellipsoid, the inertia matching ellipsoid [14] was proposed to characterize the dynamic torque-force transmission efficiency. Dynamic capability equations [15] were provided as a description of robot acceleration and force capabilities, which refers to a manipulator's ability to accelerate its end-effector and to apply forces to the environment at the end-effector.

In addition, there are many researches about configuration control of redundant manipulators discussing how to use the redundancy. Within the global methods, a time-optimal control scheme for kinematically redundant manipulators has been presented to track a predefined geometric path, subjected to joint torque limits [16], and kinematic failure tolerance has been analyzed in the environment with obstacles [17]. In Ref. [18], Ahuactzin and Gupta have proposed a global method (Kinematic Roadmap) to find a series of reachable configurations (a feasible path) from a given initial configuration to goal position based on a concept of "reachability". Within the local methods, which controls robot's configuration with limited information about environments and so on, various approaches to obstacle avoidance for redundant manipulators have been presented [19–22] including real-time control methods to avoid singular configurations [23].

Above researches indicate that the focuses on research topics concerning redundant manipulators have been shifted from kinematical consideration into combined arguments of kinematics with dynamics. What we want to emphasize is that they were based on an implicit assumption that multiple reconfiguration motions could be realized. Please note that "reconfiguration" in this paper is used for shape-changing motion of the manipulator, while the end-effector tracks a predetermined desired pose with designated dimension. Yet, whatever the choice for the secondary task, it may not necessarily lead to complete the desired internal motion, depending on the manipulator's configuration, even
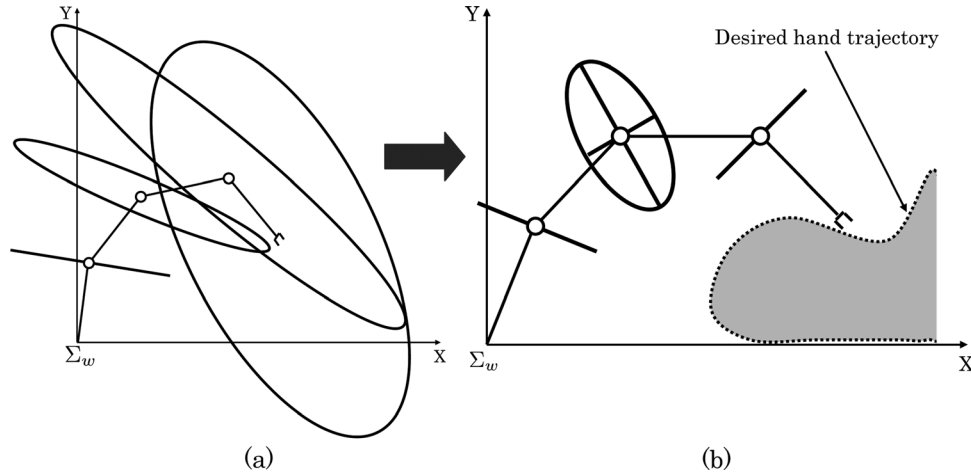
Fig. 1 Manipulability ellipsoids and reconfiguration manipulability ellipsoids

though the feasibility of the second or third reconfiguration subtasks is fully evaluated before execution. Though dozens of paper have been published on the subject, none of them has yet to analyze the feasibility of the reconfiguration subtasks.

On the other hand, the mobility of the end-effector can be evaluated by manipulability, e.g., Ref. [1] and it represents a kind of distance from singular configuration of manipulator. Contrarily to above end-effector's free motion, there has been no concept to describe reconfiguration manipulability for the secondary subtasks with prior end-effector task. We had presented a concept of the avoidance manipulability ellipsoid as an index evaluating shape-changeability of the intermediate links [24], while the end-effector tracks the desired trajectory as shown in Fig. 1(b), which is inspired from the manipulability concept [1] as shown in Fig. 1(a). The reconfiguration manipulability ellipsoids are depicted at the first and third links as partial reconfiguration manipulability ellipsoids in Fig. 1(b), and at the second link as complete reconfiguration manipulability ellipsoid, which defines the reconfiguration space of intermediate links under the predefined end-effector task. What we want to discuss here is how to guarantee and maintain the expansion of the reconfiguration space to secure a dimension of the reconfiguration space as high as possible.

Through analyses of reconfiguration matrix, the reconfiguration ability has been closely examined, and in this paper we propose:

- Reconfiguration manipulability concept to analyze and measure shape-changeability of the intermediate links providing a prior end-effector task is given.
- Through analysis of reconfiguration matrices, whether multiple reconfiguration subtasks can be executed or not, and how many subtasks are realizable can be judged on-line.
- We confirm the proposed analyses can be useful practically for evaluating the realistic manipulator's configurations and structures.
- The sufficient conditions have been shown that it can prove mathematically the sustainability of the reconfiguration space of intermediate links by nonsingular decomposition analyses of reconfiguration matrices.

Based on the above proposals, the realizability of any reconfiguration subtasks commanded by higher motion controller can be evaluated on-line. On top of it, to enable the realizable reconfiguration subtask space to spread as global as possible, what conditions can guarantee the sustainability of realizable subtask's space dimension is important since the conditions can be a criterion to control manipulator's configuration to certify and maintain expansion of the reconfiguration manipulability space. All above main points discussed are exemplified through 4-link and 7-link redundant manipulators. Finally, we discuss that a possible development of the proposed reconfiguration manipulability concept for a humanoid robot that has a primary task to control the head pose to some object by visual servoing with other subordinate tasks of the whole body stabilizing to keep standing.

2 Manipulability

2.1 Redundant Manipulator's Kinematics. Providing $m < n$ as a redundancy condition discussed in this paper, and $\dot{\boldsymbol{r}}_i = [\dot{\boldsymbol{p}}_{i+1}^T, \boldsymbol{\omega}_i^T]^T \in R^6$ where $\dot{\boldsymbol{p}}_{i+1} \in R^3$ represents linear velocity of the end of the ith link, $\boldsymbol{\omega}_i \in R^3$ represents angular velocity of the ith link, it can be written as

$$\dot{\boldsymbol{r}}_i = \boldsymbol{J}_i \dot{\boldsymbol{q}}_n \tag{1}$$

Since $\boldsymbol{q}_i = [q_1, \ldots, q_i, 0, \ldots, 0]^T (i = 1, 2, \ldots, n), \boldsymbol{J}_i$ can be described with zero block matrix

$$\boldsymbol{J}_i = [\widetilde{\boldsymbol{J}}_i, \boldsymbol{0}] \tag{2}$$

When the task space of end-effector's required motion is less than 6, the dimension of $\dot{\boldsymbol{r}}_i(\boldsymbol{q}_i)$ has also the same value.

2.2 Manipulability Ellipsoid. Considering a set of tip velocities $\dot{\boldsymbol{r}}_i$ of all links being realizable by a set of joint angle velocities $\dot{\boldsymbol{q}}_i$ that satisfies an Euclidean norm condition, that is, $\|\dot{\boldsymbol{q}}_i\| = (\dot{q}_1^2 + \dot{q}_2^2 + \cdots + \dot{q}_i^2)^{1/2} \leq 1$, then the each tip velocity shapes an ellipsoid in range space of $\boldsymbol{J}_i$. These ellipsoids have been known as "manipulability ellipsoid" [1,2], which are described as

$$\dot{\boldsymbol{r}}_i^T (\boldsymbol{J}_i^+)^T \boldsymbol{J}_i^+ \dot{\boldsymbol{r}}_i \leq 1, \quad \dot{\boldsymbol{r}}_i \in R(\boldsymbol{J}_i) \tag{3}$$

In (3), $\boldsymbol{J}_i^+$ is pseudo-inverse of $\boldsymbol{J}_i$, and $R(\boldsymbol{J}_i)$ represents range space of $\boldsymbol{J}_i$.

2.3 Manipulability Measure. Representing the volume of the "manipulability ellipsoid" of the ith link as S_{Mi}, "manipulability measure" S_M is defined as

$$S_M = \sum_{i=1}^{n} S_{Mi} \tag{4}$$

3 Reconfiguration Manipulability

Here, we assume that the desired end-effector's trajectory $\boldsymbol{r}_{nd}$ and the velocity $\dot{\boldsymbol{r}}_{nd}$ are given as primary task. Giving $i = n$ into Eq. (1), the desired $\dot{\boldsymbol{r}}_n$ is denoted by $\dot{\boldsymbol{r}}_{nd}$, then

$$\dot{\boldsymbol{r}}_{nd} = \boldsymbol{J}_n \dot{\boldsymbol{q}}_n \tag{5}$$

Solving $\dot{\boldsymbol{q}}_n$ in Eq. (5) as

$$\dot{\boldsymbol{q}}_n = \boldsymbol{J}_n^+ \dot{\boldsymbol{r}}_{nd} + (\boldsymbol{I}_n - \boldsymbol{J}_n^+ \boldsymbol{J}_n)^1 \boldsymbol{l} \qquad (6)$$

In above equation, $\boldsymbol{I}_n$ is $n \times n$ unit matrix, and $^1\boldsymbol{l}$ is an arbitrary vector satisfying $^1\boldsymbol{l} \in R^n$. The left superscript "1" of $^1\boldsymbol{l}$ means the first reconfiguration subtask. In the right side of Eq. (6), the first term denotes the solution making $\|\dot{\boldsymbol{q}}_n\|$ minimize in the null space of $\boldsymbol{J}_n$ while realizing $\dot{\boldsymbol{r}}_{nd}$. The second term denotes the components of angular velocities at each joint, which can change the manipulator's shape regardless with the influence of $\dot{\boldsymbol{r}}_{nd}$ given arbitrarily as end-effector velocity for tracking the desired trajectory. Providing the first reconfiguration subtask, which is the first demanded velocity $^1\dot{\boldsymbol{r}}_{id}$, is given to the ith link by geometric relation of manipulator and obstacles, shall we discuss realizability of $^1\dot{\boldsymbol{r}}_{id}$ in the following argument. In this research, $^1\dot{\boldsymbol{r}}_{id}$ is assumed to be commanded by an reconfiguration control system of higher level and $^1\dot{\boldsymbol{r}}_{id}$ can be used for general reconfiguration subtask. The relation of $^1\dot{\boldsymbol{r}}_{id}$ and $\dot{\boldsymbol{r}}_{nd}$ is denoted in Eq. (7) by substituting Eq. (6) into $^1\dot{\boldsymbol{r}}_{id} = \boldsymbol{J}_i \dot{\boldsymbol{q}}_n$

$$^1\dot{\boldsymbol{r}}_{id} = \boldsymbol{J}_i \boldsymbol{J}_n^+ \dot{\boldsymbol{r}}_{nd} + \boldsymbol{J}_i (\boldsymbol{I}_n - \boldsymbol{J}_n^+ \boldsymbol{J}_n)^1 \boldsymbol{l} \qquad (7)$$

Here, we define two variables shown as

$$\Delta^1\dot{\boldsymbol{r}}_{id} \overset{\Delta}{=} {}^1\dot{\boldsymbol{r}}_{id} - \boldsymbol{J}_i \boldsymbol{J}_n^+ \dot{\boldsymbol{r}}_{nd} \qquad (8)$$

and

$$^1\boldsymbol{M}_i \overset{\Delta}{=} \boldsymbol{J}_i (\boldsymbol{I}_n - \boldsymbol{J}_n^+ \boldsymbol{J}_n) \qquad (9)$$

In Eq. (8), $\Delta^1\dot{\boldsymbol{r}}_{id}$ is called by "the first reconfiguration velocity". In Eq. (9), $^1\boldsymbol{M}_i$ is a $m \times n$ matrix called by "the first reconfiguration matrix". Then, Eq. (8) can be rewritten as

$$\Delta^1\dot{\boldsymbol{r}}_{id} = {}^1\boldsymbol{M}_i^1 \boldsymbol{l} \qquad (10)$$

The relation between $^1\dot{\boldsymbol{r}}_{id}$ and $\Delta^1\dot{\boldsymbol{r}}_{id}$ is shown in Fig. 2.

Recipe:

Providing primarily given end-effector task $\dot{\boldsymbol{r}}_{nd}$ and the first reconfiguration subtask of the ith link $^1\dot{\boldsymbol{r}}_{id}$, $\Delta^1\dot{\boldsymbol{r}}_{id}$ is determined by Eq. (8). Then the realizability of $^1\dot{\boldsymbol{r}}_{id}$ depends on $rank(^1\boldsymbol{M}_i)$, meaning whether $\Delta^1\dot{\boldsymbol{r}}_{id}$ has a solution $^1\boldsymbol{l}$ through $^1\boldsymbol{M}_i$ in Eq. (10) relies on $rank(^1\boldsymbol{M}_i)$.

3.1 Complete Reconfiguration Manipulability Ellipsoid.
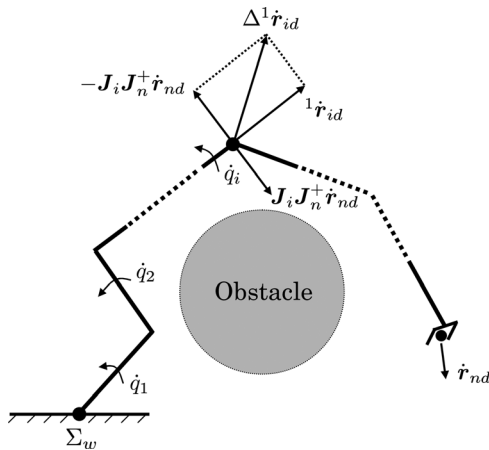When $^1\dot{\boldsymbol{r}}_{id}$ is given as the desired reconfiguration velocity of the

Fig. 2   Obstacle avoidance of intermediate links

ith link, according to Eq. (8), we can obtain $\Delta^1\dot{\boldsymbol{r}}_{id}$. However, the problem is whether we can realize $\Delta^1\dot{\boldsymbol{r}}_{id}$, that is, whether we can find $^1\boldsymbol{l}$ to realize $\Delta^1\dot{\boldsymbol{r}}_{id}$. From Eq. (10), we can obtain $^1\boldsymbol{l}$ as

$$^1\boldsymbol{l} = {}^1\boldsymbol{M}_i^+ \Delta^1\dot{\boldsymbol{r}}_{id} + (\boldsymbol{I}_n - {}^1\boldsymbol{M}_i^{+1}\boldsymbol{M}_i)^2 \boldsymbol{l} \qquad (11)$$

In Eq. (11), $^2\boldsymbol{l}$ is an arbitrary vector satisfying $^2\boldsymbol{l} \in R^n$. From Eq. (11), we can obtain

$$\|^1\boldsymbol{l}\|^2 \geq \Delta^1\dot{\boldsymbol{r}}_{id}^T (^1\boldsymbol{M}_i^+)^{T1} \boldsymbol{M}_i^+ \Delta^1\dot{\boldsymbol{r}}_{id} \qquad (12)$$

Assuming that $^1\boldsymbol{l}$ is restricted as $\|^1\boldsymbol{l}\| \leq 1$, then we obtain next relation

$$\Delta^1\dot{\boldsymbol{r}}_{id}^T (^1\boldsymbol{M}_i^+)^{T1} \boldsymbol{M}_i^+ \Delta^1\dot{\boldsymbol{r}}_{id} \leq 1, \quad \Delta^1\dot{\boldsymbol{r}}_{id} \in R(^1\boldsymbol{M}_i) \qquad (13)$$

If $rank(^1\boldsymbol{M}_i) = m$, Eq. (13) represents an ellipsoid expanding in m-dimensional space, holding

$$\Delta^1\dot{\boldsymbol{r}}_{id} = {}^1\boldsymbol{M}_i^1 \boldsymbol{M}_i^+ \Delta^1\dot{\boldsymbol{r}}_{id}, \Delta^1\dot{\boldsymbol{r}}_{id} \in R^m \qquad (14)$$

which indicates that $\Delta^1\dot{\boldsymbol{r}}_{id}$ can be arbitrarily realized in m-dimensional space and Eq. (10) always has the solution $^1\boldsymbol{l}$ corresponding to all $\Delta^1\dot{\boldsymbol{r}}_{id} \in R^m$. In this way, the ellipsoid represented by Eq. (13) when $rank(^1\boldsymbol{M}_i) = m$ is named "the first complete reconfiguration manipulability ellipsoid", which is denoted by $^{1C}P_i$.

3.2 Partial Reconfiguration Manipulability Ellipsoid.
If $rank(^1\boldsymbol{M}_i) = p < m$, $\Delta^1\dot{\boldsymbol{r}}_{id}$ does not value arbitrarily in R^m. In this case, reduced $\Delta^1\dot{\boldsymbol{r}}_{id}$ is denoted as $\Delta^1\dot{\boldsymbol{r}}_{id}^*$. Then Eq. (13) is written as

$$\Delta^1\dot{\boldsymbol{r}}_{id}^{*^T} (^1\boldsymbol{M}_i^+)^{T1} \boldsymbol{M}_i^+ \Delta^1\dot{\boldsymbol{r}}_{id}^* \leq 1,$$
$$(\Delta^1\dot{\boldsymbol{r}}_{id}^* = {}^1\boldsymbol{M}_i^1 \boldsymbol{M}_i^+ \boldsymbol{s}, \quad \boldsymbol{s} \in R^m) \qquad (15)$$

Above equation describes an ellipsoid expanded in p-dimensional space. This ellipsoid is named "the first partial reconfiguration manipulability ellipsoid," which is denoted by $^{1P}P_i$. Because $p < m$, the partial reconfiguration manipulability ellipsoid can be thought as regressed ellipsoid of the complete reconfiguration manipulability ellipsoid. We call ^1P_i as the first reconfiguration manipulability ellipsoid including both $^{1C}P_i$ and $^{1P}P_i$.

According to above analysis, we can generalize as follows.

LEMMA 1. *The necessary and sufficient condition of Eq. (14) being held for all $\Delta^1\dot{\boldsymbol{r}}_{id} \in R^m$ is $rank(^1\boldsymbol{M}_i) = m$.*

Proof of Lemma 1. (necessary condition)

According to Eq. (14), when $(\boldsymbol{I}_m - {}^1\boldsymbol{M}_i^1\boldsymbol{M}_i^+)\Delta^1\dot{\boldsymbol{r}}_{id} = \boldsymbol{0}$ holds for all $\Delta^1\dot{\boldsymbol{r}}_{id} \in R^m$, it is necessary that $^1\boldsymbol{M}_i^1\boldsymbol{M}_i^+ = \boldsymbol{I}_m$. Then $^1\boldsymbol{M}_i \in R^{m \times n}$ should be row full rank, that is, $rank(^1\boldsymbol{M}_i) = m$.

(sufficient condition)

Since $rank(^1\boldsymbol{M}_i) = m$, $^1\boldsymbol{M}_i$ has m nonzero singular values $(\sigma_1, \sigma_2, ..., \sigma_m)$. Then, $^1\boldsymbol{M}_i$ can be decomposed by $^1\boldsymbol{M}_i = \boldsymbol{U}_i \boldsymbol{\Sigma}_i \boldsymbol{V}_i^T$, where $\boldsymbol{U}_i$ is the $m \times m$ unit orthogonal matrix satisfying $\boldsymbol{U}_i \boldsymbol{U}_i^T = \boldsymbol{U}_i^T \boldsymbol{U}_i = \boldsymbol{I}_m, \boldsymbol{\Sigma}_i = (diag(\sigma_k)|\boldsymbol{0})$ $(k = 1, ..., m$ and $\sigma_k \neq 0)$ and $\boldsymbol{V}_i$ is the $n \times n$ unit orthogonal matrix satisfying $\boldsymbol{V}_i \boldsymbol{V}_i^T = \boldsymbol{V}_i^T \boldsymbol{V}_i = \boldsymbol{I}_n$. In addition, $^1\boldsymbol{M}_i^+ = \boldsymbol{V}_i \boldsymbol{\Sigma}_i^+ \boldsymbol{U}_i^T$, where $\boldsymbol{\Sigma}_i^+ = (diag(\sigma_k^{-1})|\boldsymbol{0})^T$ $(k = 1, ..., m$ and $\sigma_k \neq 0)$. In this way, Eq. (14) follows from $^1\boldsymbol{M}_i^1\boldsymbol{M}_i^+ = \boldsymbol{U}_i \boldsymbol{\Sigma}_i \boldsymbol{V}_i^T \boldsymbol{V}_i \boldsymbol{\Sigma}_i^+ \boldsymbol{U}_i^T = \boldsymbol{I}_m$.

LEMMA 2. *If $rank(^1\boldsymbol{M}_i) = p < m$, $\Delta^1\dot{\boldsymbol{r}}_{id} \in R^m$ does not always satisfy Eq. (14). But the orthogonal projection of $\Delta^1\dot{\boldsymbol{r}}_{id}$ onto $R(^1\boldsymbol{M}_i)$, that is, all $\Delta^1\dot{\boldsymbol{r}}_{id}^* \in R(^1\boldsymbol{M}_i)$ can be realized.*

Proof of Lemma 2. From "**Lemma 1**" and relation shown in Eq. (15), "**Lemma 2**" is proved.

THEOREM 1. *All $^1\dot{\boldsymbol{r}}_{id} \in R^m$ can be realized for any $\dot{\boldsymbol{r}}_{nd}$ being given primarily as the end-effector task, if and only if $rank(^1\boldsymbol{M}_i) = m$.*

Proof of Theorem 1. From "**Lemma 1,**" Eqs. (8) and (10), "**Theorem 1**" follows.

THEOREM 2. *If* $rank(^1M_i) = p < m$, *it is not that all* $^1\dot{r}_{id} \in R^m$ *can be realized. But*

$$^1\dot{r}_{id}^\sharp \overset{\Delta}{=} \Delta^1\dot{r}_{id}^* + J_i J_n^+ \dot{r}_{nd} \qquad (16)$$

can be realized since $\Delta^1\dot{r}_{id}^* \in R(^1M_i)$ *in dimension p, that is* $^1\dot{r}_{id}^\sharp$ *is contained in the affine space*

$$R(^1M_i) + J_i J_n^+ \dot{r}_{nd} \qquad (17)$$

whose dimension is also p.

Proof of Theorem 2. From "Lemma 2," Eqs. (8) and (10), "Theorem 2" follows.

3.3 Reconfiguration Manipulability Measure.

Representing the volume of the "reconfiguration manipulability ellipsoid" of the ith link as S_{RMi}, "reconfiguration manipulability measure" S_{RM} is defined as

$$S_{RM} = \sum_{i=1}^{n-1} S_{RMi} \qquad (18)$$

where S_{RM} is similar with ^1E shown in Eq. (16) in Ref. [28]. S_{RMi} is similar with $^1V_i a_i$ defined in Eqs. (13)–(17) in Ref. [28].

4 Plural Reconfiguration Subtasks

In Sec. 3, we defined the first reconfiguration manipulability ellipsoid $^1P_i (i = 1, ..., n - 1)$. However, in fact, it may not be possible that these intermediate links realize their own reconfiguration velocities simultaneously. That is whether $\Delta^1\dot{r}_{id}$ and $\Delta^1\dot{r}_{jd} (i \neq j)$ satisfying $\Delta^1\dot{r}_{id} = {}^1M_i^1 l$ and $\Delta^1\dot{r}_{jd} = {}^1M_j^1 l$ can be realized simultaneously is not guaranteed. This section discusses the multireconfiguration subtasks realization. If the first reconfiguration subtask, that is, the first reconfiguration velocity, $\Delta^1\dot{r}_{id}$ or $\Delta^1\dot{r}_{id}^*$ has been realized at a certain ith link, we will consider the possibility to execute the second reconfiguration velocity except the ith link. Substituting Eq. (11) into Eq. (6), we can obtain

$$\dot{q}_n = J_n^+ \dot{r}_{nd} + (I_n - J_n^+ J_n)^1 M_i^+ \Delta^1 \dot{r}_{id}$$
$$+ (I_n - J_n^+ J_n)(I_n - {}^1M_i^{+1}M_i)^2 l \qquad (19)$$

Substituting Eq. (19) into $^2\dot{r}_{jd} = J_j \dot{q}_n$, we can obtain

$$^2\dot{r}_{jd} = J_j J_n^+ \dot{r}_{nd} + J_j(I_n - J_n^+ J_n)^1 M_i^+ \Delta^1 \dot{r}_{id}$$
$$+ J_j(I_n - J_n^+ J_n)(I_n - {}^1M_i^{+1}M_i)^2 l \qquad (20)$$

By defining $\Delta^2\dot{r}_{jd}$ and ^2M_j as

$$\Delta^2\dot{r}_{jd} \overset{\Delta}{=} {}^2\dot{r}_{jd} - J_j J_n^+ \dot{r}_{nd} - J_j(I_n - J_n^+ J_n)^1 M_i^+ \Delta^1 \dot{r}_{id} \qquad (21)$$

and

$$^2M_j \overset{\Delta}{=} J_j(I_n - J_n^+ J_n)(I_n - {}^1M_i^{+1}M_i) \qquad (22)$$

we can obtain

$$\Delta^2\dot{r}_{jd} = {}^2 M_j^2 l \qquad (23)$$

The forms of Eqs. (23) and (10) are similar. Therefore, the analysis method of the second reconfiguration manipulability ellipsoid $^2P_j(j = 1, ..., n - 1; \{j \neq i\})$ and the first reconfiguration manipulability ellipsoid ^1P_i are also similar. In other words, whether the

second reconfiguration subtask can be realized or not depends on the rank value of second matrix $^2M_j(j = 1, ..., n - 1; \{j \neq i\})$. If $rank(^2M_j) \neq 0$, the second subtask can be realized partially at least. If $rank(^2M_j) = 0$, the second reconfiguration subtask cannot be realized. Similarly, we can judge whether the third subtask can be realized or not by the third reconfiguration matrix ^3M_k as

$$^3M_k \overset{\Delta}{=} J_k(I_n - J_n^+ J_n)(I_n - {}^1M_i^{+1}M_i)(I_n - {}^2M_j^{+2}M_j),$$
$$(k = 1, ..., n - 1; \{k \neq i\} \cap \{k \neq j\} \cap \{i \neq j\}) \qquad (24)$$

According to above analyses for $^1M_i, {}^2M_j$, and ^3M_k, the realizability of the fourth or more subtasks can be judged in a same manner.

Here, we show judgment sequence by a flow chart shown in Fig. 3 when β reconfiguration subtasks are demanded. i denotes the number of link, $\alpha(\alpha = 1, 2, ..., \beta)$ denotes the priority order of reconfiguration subtasks, $^\alpha\dot{r}_{id}$ means the arbitrarily demanded reconfiguration velocity for the ith link as the αth reconfiguration subtask. According to Fig. 3, whether the arbitrary $^\alpha\dot{r}_{id}$ and the end-effector velocity $\dot{r}_{nd}$ are both realized or not can be judged through $\Delta^\alpha\dot{r}_{id}$ recurrently.

5 Analysis of $rank(^1M_i)$

Maintaining $rank(^1M_i)$ of intermediate links to be as high as possible is the essential requirement for configuration control to optimize manipulator's shape in view of high reconfiguration manipulability. And it is the first step to design an on-line control system of a redundant manipulator with high shape-changeability based on reconfiguration manipulability. We want to stress here previous researches have not paid attention to how to guarantee $rank(^1M_i)$ to assure the required avoiding task to be realizable. In fact, a similar concept of ^1M_i had initially been defined and used for controlling the redundant manipulator's configuration based on prioritized multiple tasks [25]. However, the proposed controller in Ref. [25] do not concern the possibility that the range space of ^1M_i could be reduced by singular configuration and it cannot decouple the interacting motions of multiple tasks even though the redundant degree be much higher than the required motion degree of the multiple tasks. Even in our previous researches about avoidance manipulability optimization [26] and on-line control system [27,28] of a redundant manipulator, we did not guarantee the sustainability of the range space of ^1M_i. In this
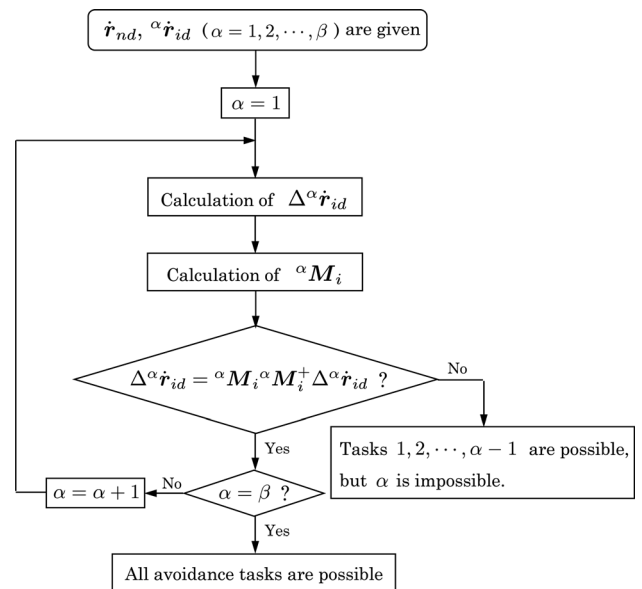

Fig. 3 Flow chart of judgment of reconfiguration possibility

section, we will propose three assumptions named as "Practical Configuration Assumption," "Nonsingular Configuration Assumption" and "Full-Nonsingular Configuration Assumption," they can provide a configuration control criterion as primary control objective to keep the shape-changeability by avoiding singular configuration.

5.1 Mathematical Descriptions

5.1.1 Mathematical Definitions. When $rank(J_n) = m, J_n$ can be decomposed by

$$J_n = U\Sigma V^T \tag{25}$$

and J_n^+ can be decomposed by

$$J_n^+ = V\Sigma^+ U^T \tag{26}$$

In Eqs. (25) and (26), U is $m \times m$ orthogonal matrix satisfying $UU^T = U^T U = I_m$, V is $n \times n$ orthogonal matrix satisfying $VV^T = V^T V = I_n$, Σ is $m \times n$ matrix, which includes a diagonal matrix composing of m nonzero singular values of J_n and the rest parts are all zero elements. Σ^+ is $n \times m$ matrix.

Generally, V can be defined with column vectors $\hat{v}_i (i = 1, 2, ..., n)$ by

$$V = [\hat{v}_1, \hat{v}_2, ..., \hat{v}_n] \tag{27}$$

V can be redefined with row vectors $\check{v}_i \ (i = 1, 2, ..., n)$ by

$$V = \begin{bmatrix} \check{v}_1 \\ \check{v}_2 \\ \vdots \\ \check{v}_n \end{bmatrix} \tag{28}$$

In addition, we know that J_n can be also decomposed by

$$J_n = U_m \Sigma_m V_m^T \tag{29}$$

and J_n^+ can be decomposed by

$$J_n^+ = V_m \Sigma_m^+ U_m^T \tag{30}$$

In Eqs. (29) and (30), U_m is $m \times m$ matrix satisfying $U_m U_m^T = U_m^T U_m = I_m$, V_m^T is $m \times n$ matrix satisfying $V_m^T V_m = I_m$, Σ_m is $m \times m$ matrix, which is a diagonal matrix including m nonzero singular values of J_n. Σ_m^+ is also $m \times m$ diagonal matrix.

According to above discussion, we can clearly obtain the relations of U and U_m, V and V_m, Σ and Σ_m, Σ^+ and Σ_m^+ as

$$\begin{cases} U = U_m \\ V = [V_m, \quad V_{n-m}] \\ \Sigma = [\Sigma_m, \quad 0] \\ \Sigma^+ = \begin{bmatrix} \Sigma_m^+ \\ 0 \end{bmatrix} \end{cases} \tag{31}$$

In above equation, V_m is defined using first m column vectors $\hat{v}_j \ (j = 1, 2, ..., m)$ in Eq. (27) as

$$V_m = [\hat{v}_1, ..., \hat{v}_m] \tag{32}$$

where V_m is redefined referring to row vectors $\check{v}_i \ (i = 1, 2, ..., n)$ in Eq. (28) as

$$V_m = \begin{bmatrix} \check{v}_{1,m} \\ \vdots \\ \check{v}_{n,m} \end{bmatrix} \tag{33}$$

where V_{n-m} is the rest block part of V except V_m. So, V_{n-m} can be denoted using column vectors $\hat{v}_j \ (j = m+1, ..., n)$ in Eq. (27) as

$$V_{n-m} = [\hat{v}_{m+1}, ..., \hat{v}_n] \tag{34}$$

where V_{n-m} can be redenoted referring to row vectors $\check{v}_i \ (i = 1, 2, ..., n)$ in Eq. (28) as

$$V_{n-m} = \begin{bmatrix} \check{v}_{1,(n-m)} \\ \vdots \\ \check{v}_{n,(n-m)} \end{bmatrix} \tag{35}$$

We can divide V_{n-m} as

$$V_{n-m} = \begin{bmatrix} V_{i,(n-m)} \\ V_{(n-i),(n-m)} \end{bmatrix} \tag{36}$$

In Eq. (36), $V_{i,(n-m)}$ is

$$V_{i,(n-m)} = \begin{bmatrix} \check{v}_{1,(n-m)} \\ \vdots \\ \check{v}_{i,(n-m)} \end{bmatrix} \tag{37}$$

and $V_{(n-i),(n-m)}$ is

$$V_{(n-i),(n-m)} = \begin{bmatrix} \check{v}_{(i+1),(n-m)} \\ \vdots \\ \check{v}_{n,(n-m)} \end{bmatrix} \tag{38}$$

Then, if we divide V_m into two block matrices ($V_{(n-m),m}$ and $V_{m,m}$) and divide V_{n-m} into two block matrices ($V_{(n-m),(n-m)}$ and $V_{m,(n-m)}$). Therefore, V can be redenoted by

$$\begin{aligned} V &= [V_m, V_{n-m}] \\ &= \begin{bmatrix} V_{(n-m),m} & V_{(n-m),(n-m)} \\ V_{m,m} & V_{m,(n-m)} \end{bmatrix} \end{aligned} \tag{39}$$

5.1.2 The First Reconfiguration Matrix. Here, we have defined the first reconfiguration matrix ${}^1M_i \ (i = 1, 2, ..., n-1)$ as (9). Here, ${}^1M_i$ is redefined as

$${}^1M_i = J_i L_n \tag{40}$$

where

$$L_n = I_n - J_n^+ J_n \tag{41}$$

5.1.3 Decomposition of L_n. If $rank(J_n) = m$. Then, according to Eqs. (25) and (26) and referring to Eq. (39), L_n can be decomposed by

$$L_n = V_{n-m} V_{n-m}^T \tag{42}$$

In above equation, because $rank(V_{n-m}) = rank(V_{n-m}^T) = n - m$, we can obtain
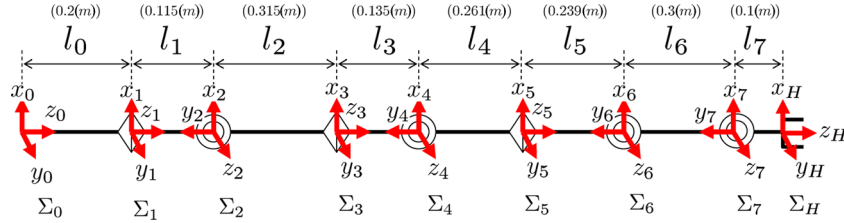
Fig. 4 Structure of PA11

$$rank(\boldsymbol{L}_n) = n - m \tag{43}$$

The above decomposition of $\boldsymbol{L}_n$ is a preparation for the decomposition of ${}^1\boldsymbol{M}_i$, following in Sec. 5.2.

5.2 Description of $rank({}^1\boldsymbol{M}_i)$. Proofs of "**Propositions**," "**Lemmas**," "**Theorems**," and "**Corollaries**" in this subsection are all given in "**Appendix**".

PROPOSITION a. $rank({}^1\boldsymbol{M}_n) = 0$, *since* ${}^1\boldsymbol{M}_n = \boldsymbol{0}$.

This means that the end-effector of the manipulator does not possess the reconfiguration manipulability.

PROPOSITION b. *When* $1 \leq i \leq n - 1$, *according to Eqs.* (2), (36), *and* (42), ${}^1\boldsymbol{M}_i$ *can be decomposed as*

$$ {}^1\boldsymbol{M}_i = \tilde{\boldsymbol{J}}_i \boldsymbol{V}_{i,(n-m)} \boldsymbol{V}_{n-m}^T \tag{44}$$

which leads to

$$ rank(\tilde{\boldsymbol{J}}_i) + rank(\boldsymbol{V}_{i,(n-m)}) - i \leq rank({}^1\boldsymbol{M}_i) $$
$$ \leq \min\{rank(\tilde{\boldsymbol{J}}_i), rank(\boldsymbol{V}_{i,(n-m)}), n - m\} \tag{45}$$

Here, we give the definition of matrix $\boldsymbol{J}_i^{a \to b}$ ($1 \leq i \leq n$ and $1 \leq a \leq b \leq n$). From Eq. (2), we know that $\boldsymbol{J}_i$ is a $m \times n$ matrix composed of column vectors $\tilde{\boldsymbol{j}}_{ij}$ ($1 \leq j \leq i$) and $\boldsymbol{0}$ as

$$ \boldsymbol{J}_i = [\tilde{\boldsymbol{j}}_{i1}, \ldots, \tilde{\boldsymbol{j}}_{ii}, \boldsymbol{0}] \tag{46}$$

then, $\boldsymbol{J}_i^{a \to b}$ is a $m \times (b - a + 1)$ matrix, which only includes the ath to the bth column vectors of $\boldsymbol{J}_i$ as

$$ \boldsymbol{J}_i^{a \to b} = [\tilde{\boldsymbol{j}}_{ia}, \ldots, \tilde{\boldsymbol{j}}_{ib}] \tag{47}$$

In this way, $\boldsymbol{J}_n^{n-m+1 \to n}$ represents a block matrix comprising the last m column vectors of $\boldsymbol{J}_n$.

LEMMA a. *Assuming* $rank(\boldsymbol{J}_n^{n-m+1 \to n}) = m$, *we have*

$$ rank(\boldsymbol{V}_{i,(n-m)}) = \min\{i, n - m\}, \quad (1 \leq i \leq n) \tag{48}$$

$rank(\boldsymbol{J}_i) = \min\{i, m\}$ means that if $i < m$ the configuration of the 1st link to ith link is nonsingular, and if $i \geq m$ the configuration of the 1st link to ith link is nonsingular in the sense that the configuration is available for the ith link to achieve a motion in m dimension space.

5.2.1 The Practical Configuration Assumption. According to "Lemma a" and "Proposition b," we obtain the next theorem.

THEOREM a. *Giving the practical configuration assumption for any manipulator as*

$$ \begin{cases} (a). \; rank(\boldsymbol{J}_n^{n-m+1 \to n}) = m \\ (b_i). \; rank(\boldsymbol{J}_i) = p_i, \; (i = 1, 2, \ldots, n - 1) \end{cases} \tag{49}$$

with $p_i \in \{0, 1, \ldots, m\}$, we have

$$ p_i + \min\{i, n - m\} - i \leq rank({}^1\boldsymbol{M}_i) \leq \min\{p_i, i, n - m\} \tag{50}$$

The assumption (a) in Eq. (49) represents that the configuration from the $(n - m)$th link to the nth link is nonsingular. The next assumption (b_i) is affected by many factors such as the structure of manipulator, variables choice of end-effector task and manipulator's configuration and so on, so $rank(\boldsymbol{J}_i)$ is given by an unspecified value p_i to make the assumption be practical. For verifying the practicality of concept of reconfiguration manipulability, here we use our original robot named "PA11" to evaluate reconfiguration manipulability ellipsoid. "PA11" is a 7-link redundant manipulator ($n = 7$) and its end-effector can execute the task in three-dimensional position space ($m = 3$). The structure of "PA11" is shown in Fig. 4, where all joints are rotational and their rotational directions are given by z-axis of each link coordinate z_i. Considering the structure of "PA11", and assuming that the end-effector of "PA11" executes the task in three-dimensional position space, that is $\boldsymbol{p}_i = [x, y, z]^T$. When "PA11" is set by $q_1 = 0$ deg, $q_2 = -90$ deg, $q_3 = 0$ deg, $q_4 = 90$ deg, $q_5 = 0$ deg, $q_6 = -90$ deg, and $q_7 = 90$ deg shown in Fig. 5(*a*), we can simply find that the conditions in Eq. (49) given as

$$ \begin{cases} rank(\boldsymbol{J}_7^{5 \to 7}) = 3 \\ rank(\boldsymbol{J}_1) = 0 \\ rank(\boldsymbol{J}_2) = rank(\boldsymbol{J}_3) = 2 \\ rank(\boldsymbol{J}_4) = rank(\boldsymbol{J}_5) = rank(\boldsymbol{J}_6) = 3 \end{cases} \tag{51}$$

with

$$ \boldsymbol{J}_7^{5 \to 7} = \begin{bmatrix} 0 & 0.1 & 0.1 \\ -0.3 & 0 & 0 \\ 0 & 0.3 & 0 \end{bmatrix} \tag{52}$$

Substituting Eq. (51) into Eq. (50), we can obtain

$$ \begin{cases} rank({}^1\boldsymbol{M}_1) = 0 \\ rank({}^1\boldsymbol{M}_2) = rank({}^1\boldsymbol{M}_3) = 2 \\ rank({}^1\boldsymbol{M}_4) = 3 \\ 2 \leq rank({}^1\boldsymbol{M}_5) \leq 3, \quad 1 \leq rank({}^1\boldsymbol{M}_6) \leq 3 \end{cases} \tag{53}$$
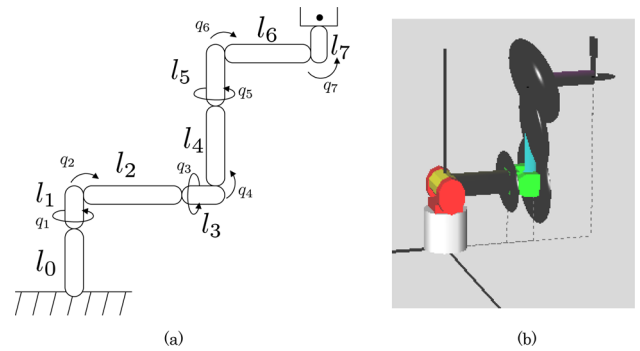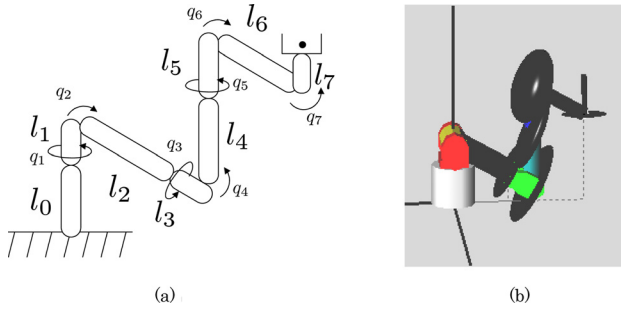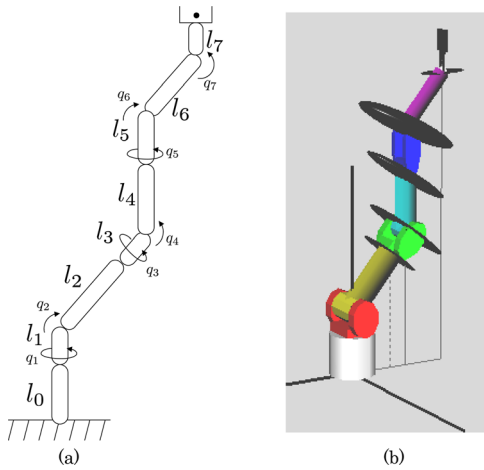

(a)   (b)

Fig. 5 Shape 1 of PA11 and reconfiguration manipulability ellipsoids ($q_1 = 0$ deg, $q_2 = -90$ deg, $q_3 = 0$ deg, $q_4 = 90$ deg, $q_5 = 0$ deg, $q_6 = -90$ deg, $q_7 = 90$ deg; $l_0 = 0.2$ m, $l_1 = 0.115$ m, $l_2 = 0.315$ m, $l_3 = 0.135$ m, $l_4 = 0.261$ m, $l_5 = 0.239$ m, $l_6 = 0.3$ m, $l_7 = 0.1$ m)
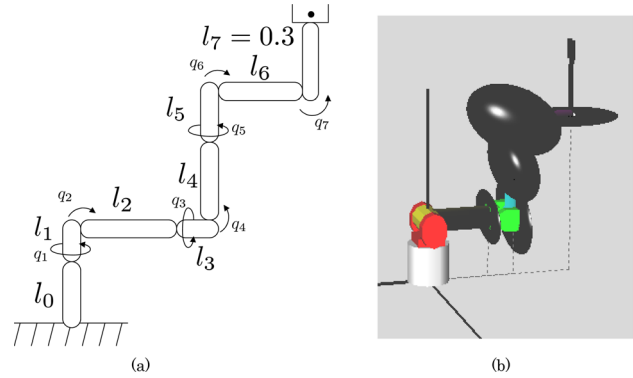
Fig. 6 Shape 2 of PA11 and reconfiguration manipulability ellipsoids ($q_1 = 0$ deg, $q_2 = -120$ deg, $q_3 = 0$ deg, $q_4 =$ deg, $q_5 = 0$ deg, $q_6 = -120$ deg, $q_7 = 120$ deg; $l_0 = 0.2$ m, $l_1 = 0.115$ m, $l_2 = 0.315$ m, $l_3 = 0.135$ m, $l_4 = 0.261$ m, $l_5 = 0.239$ m, $l_6 = 0.3$ m, $l_7 = 0.1$ m)

Fig. 7 Shape 3 of PA11 and reconfiguration manipulability ellipsoids ($q_1 = 0$ deg, $q_2 = -40$ deg, $q_3 = 0$ deg, $q_4 = 40$ deg, $q_5 = 0$ deg, $q_6 = -40$ deg, $q_7 = 40$ deg; $l_0 = 0.2$ m, $l_1 = 0.115$ m, $l_2 = 0.315$ m, $l_3 = 0.135$ m, $l_4 = 0.261$ m, $l_5 = 0.239$ m, $l_6 = 0.3$ m, $l_7 = 0.1$ m)

On the other hand, from Eq. (9) we can calculate

$$
\begin{cases}
rank(^1\boldsymbol{M}_1) = 0 \\
rank(^1\boldsymbol{M}_2) = rank(^1\boldsymbol{M}_3) = 2 \\
rank(^1\boldsymbol{M}_4) = 3 \\
rank(^1\boldsymbol{M}_5) = 3, rank(^1\boldsymbol{M}_6) = 2
\end{cases}
\tag{54}
$$

In Eq. (54), $rank(^1\boldsymbol{M}_1), rank(^1\boldsymbol{M}_2), rank(^1\boldsymbol{M}_3)$, and $rank(^1\boldsymbol{M}_4)$ are completely coincide with Eq. (53), $rank(^1\boldsymbol{M}_5)$ and $rank(^1\boldsymbol{M}_6)$ are in the extent of Eq. (53).

The reconfiguration manipulability ellipsoids given by Eq. (13) or Eq. (15) are shown in Fig. 5(*b*), where the 1st link does not possess the reconfiguration manipulability since $rank(^1\boldsymbol{M}_1) = 0$. The 2nd and 3rd links possess the reconfiguration manipulability in two-dimensional position space since $rank(^1\boldsymbol{M}_3) = rank(^1\boldsymbol{M}_4)$ $= 2$ in Eq. (54), the ellipsoids are vertical with the principal axes of the 2nd link and 3rd link, respectively, here please note that the ellipsoid of the 3rd link is somewhat larger than the ellipsoid of the 2nd link because of influence of the length of the 3rd link, that is l_3. The 4th and 5th links possess the reconfiguration manipulability in three-dimensional position space since $rank(^1\boldsymbol{M}_4) = 3$ and $rank(^1\boldsymbol{M}_5) = 3$, the 6th link possesses the reconfiguration manipulability in two-dimensional position space since $rank(^1\boldsymbol{M}_7) = 2$, which is vertical with the 7th link. These results prove the consistency between "**Theorem a**" and practice.

Fig. 8 Shape 4 of PA11 and reconfiguration manipulability ellipsoids ($q_1 = 0$ deg, $q_2 = -90$ deg, $q_3 = 0$ deg, $q_4 = 90$ deg, $q_5 = 0$ deg, $q_6 = -90$ deg, $q_7 = 90$ deg; $l_0 = 0.2$ m, $l_1 = 0.115$ m, $l_2 = 0.315$ m, $l_3 = 0.135$ m, $l_4 = 0.261$ m, $l_5 = 0.239$ m, $l_6 = 0.3$ m, $l_7 = 0.3$ m)
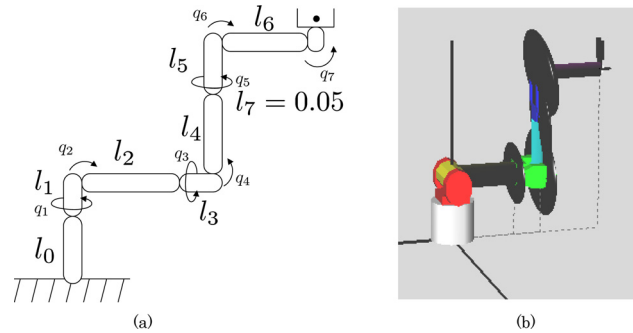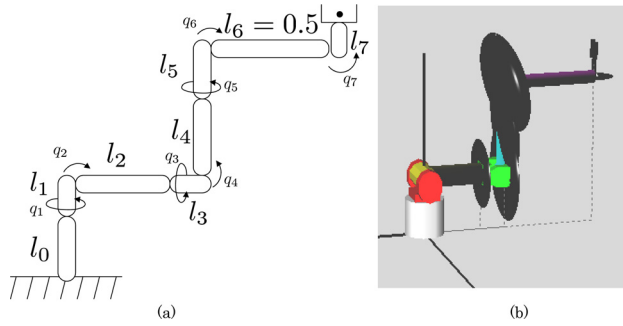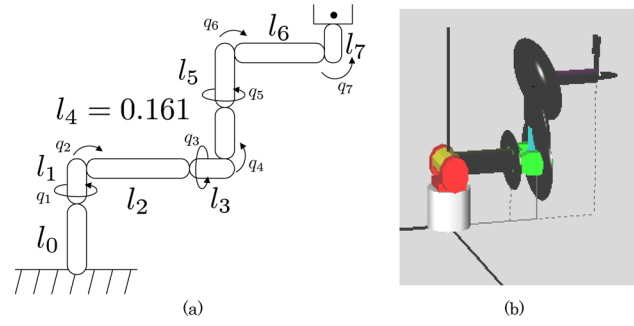

Fig. 9 Shape 5 of PA11 and reconfiguration manipulability ellipsoids ($q_1 = 0$ deg, $q_2 = -90$ deg, $q_3 = 0$ deg, $q_4 = 90$ deg, $q_5 = 0$ deg, $q_6 = -90$ deg, $q_7 = 90$ deg; $l_0 = 0.2$ m, $l_1 = 0.115$ m, $l_2 = 0.315$ m, $l_3 = 0.135$ m, $l_4 = 0.261$ m, $l_5 = 0.239$ m, $l_6 = 0.3$ m, $l_7 = 0.05$ m)

When we change the shape of "PA11" with the same structure and link length. For example, the shape is changed into $q_1 = 0$ deg, $q_2 = -120$ deg, $q_3 = 0$ deg, $q_4 = 120$ deg, $q_5 = 0$ deg, $q_6 = -120$ deg, $q_7 = 120$ deg and $q_1 = 0$ deg, $q_2 = -40$ deg, $q_3 = 0$ deg, $q_4 = 40$ deg, $q_5 = 0$ deg, $q_6 = -40$ deg, $q_7 = 40$ deg, we can find the area or volume of all ellipsoids shown in Figs. 6 and 7 decrease. Above discussions are how the manipulator's configuration affect the reconfiguration manipulability.

Next, we will discuss the reconfiguration manipulability by changing the manipulator's structure as a parameter. When we change the structure of "PA11" in length of links. For example, l_7 is increased into 0.3 m from 0.1 m, or l_6 is increased into 0.5 m from 0.3 m, or l_4 is increased into 0.561 m from 0.261 m, or l_2 is increased into 0.615 m from 0.315 m, the area and volume of the all ellipsoids will become large, which are shown in Figs. 8, 10, 12, and 14, respectively. On the contrary, when l_7 is decreased into 0.05 m from 0.1 m, or l_6 is decreased into 0.1 m from 0.3 m, or l_4 is decreased into 0.161 m from 0.261 m, or l_2 is decreased into 0.115 m from 0.315 m, the area and volume of the all ellipsoids will become small, which are shown in Figs. 9, 11, 13, and 15, respectively. In addition, from Figs. 16 and 17, we can find the change of l_0 will not affect the ellipsoids. Figures 5–17 represent how the structure affects the area and volume of ellipsoids. Here, please note that the changes of shape and structure shown from Figs. 5–17 are under the configuration given by Eq. (51). By calculations, their ellipsoids are completely coincide with Eq. (54).
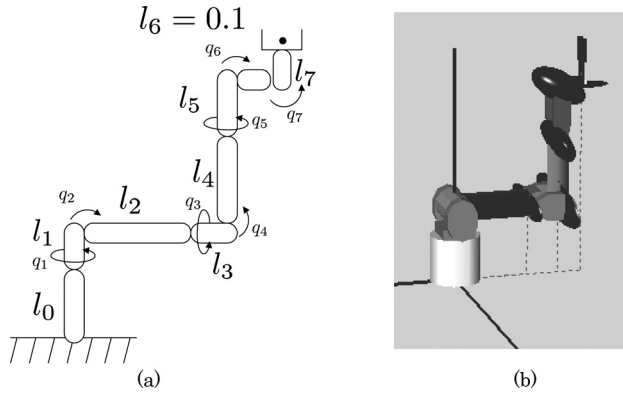
However, as shown in Fig. 18 $q_1 = 0$ deg, $q_2 = -90$ deg, $q_3 = 0$ deg, $q_4 = 90$ deg, $q_5 = 0$ deg, $q_6 = -90$ deg, $q_7 = 0$ deg, when the assumption (*a*) in Eq. (49) does not be satisfied such as $rank(\boldsymbol{J}_7{}^{5 \to 7}) = 2$ with
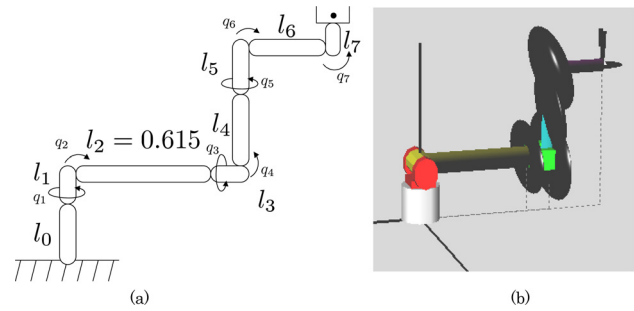
Fig. 10 Shape 6 of PA11 and reconfiguration manipulability ellipsoids ($q_1 = 0$ deg, $q_2 = -90$ deg, $q_3 = 0$ deg, $q_4 = 90$ deg, $q_5 = 0$ deg, $q_6 = -90$ deg, $q_7 = 90$ deg; $l_0 = 0.2$ m, $l_1 = 0.115$ m, $l_2 = 0.315$ m, $l_3 = 0.135$ m, $l_4 = 0.261$ m, $l_5 = 0.239$ m, $l_6 = 0.5$ m, $l_7 = 0.1$ m)
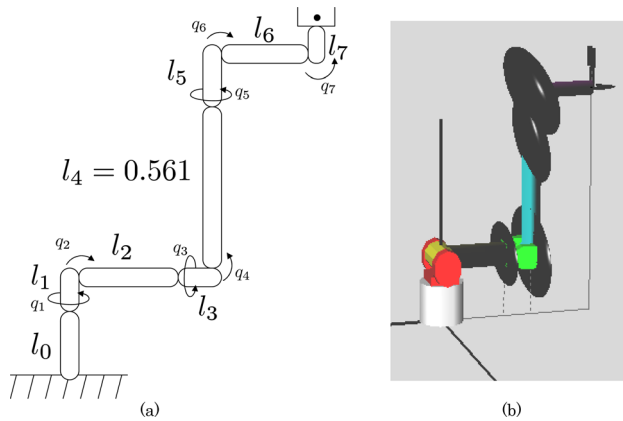

Fig. 11 Shape 7 of PA11 and reconfiguration manipulability ellipsoids ($q_1 = 0$ deg, $q_2 = -90$ deg, $q_3 = 0$ deg, $q_4 = 90$ deg, $q_5 = 0$ deg, $q_6 = -90$ deg, $q_7 = 90$ deg; $l_0 = 0.2$ m, $l_1 = 0.115$ m, $l_2 = 0.315$ m, $l_3 = 0.135$ m, $l_4 = 0.261$ m, $l_5 = 0.239$ m, $l_6 = 0.1$ m, $l_7 = 0.1$ m)

Fig. 12 Shape 8 of PA11 and reconfiguration manipulability ellipsoids ($q_1 = 0$ deg, $q_2 = -90$ deg, $q_3 = 0$ deg, $q_4 = 90$ deg, $q_5 = 0$ deg, $q_6 = -90$ deg, $q_7 = 90$ deg; $l_0 = 0.2$ m, $l_1 = 0.115$ m, $l_2 = 0.315$ m, $l_3 = 0.135$ m, $l_4 = 0.561$ m, $l_5 = 0.239$ m, $l_6 = 0.3$ m, $l_7 = 0.1$ m)
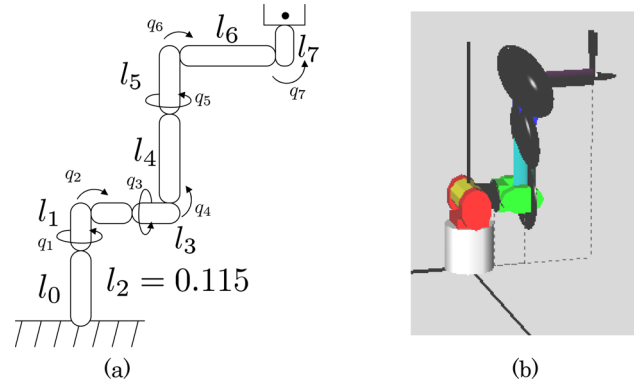
$$J_7^{5 \rightarrow 7} = \begin{bmatrix} 0 & 0 & 0 \\ -0.4 & 0 & 0 \\ 0 & 0.4 & 0.1 \end{bmatrix} \tag{55}$$

we can find the 4th link only possesses the reconfiguration manipulability in two-dimensional position space, that is

Fig. 13 Shape 9 of PA11 and reconfiguration manipulability ellipsoids ($q_1 = 0$ deg, $q_2 = -90$ deg, $q_3 = 0$ deg, $q_4 = 90$ deg, $q_5 = 0$ deg, $q_6 = -90$ deg, $q_7 = 90$deg; $l_0 = 0.2$ m, $l_1 = 0.115$ m, $l_2 = 0.315$ m, $l_3 = 0.135$ m, $l_4 = 0.161$ m, $l_5 = 0.239$ m, $l_6 = 0.3$ m, $l_7 = 0.1$ m)

Fig. 14 Shape 10 of PA11 and reconfiguration manipulability ellipsoids ($q_1 = 0$ deg, $q_2 = -90$ deg, $q_3 = 0$ deg, $q_4 = 90$ deg, $q_5 = 0$ deg, $q_6 = -90$ deg, $q_7 = 90$ deg; $l_0 = 0.2$ m, $l_1 = 0.115$ m, $l_2 = 0.615$ m, $l_3 = 0.135$ m, $l_4 = 0.261$ m, $l_5 = 0.239$ m, $l_6 = 0.3$ m, $l_7 = 0.1$ m)

Fig. 15 Shape 11 of PA11 and reconfiguration manipulability ellipsoids ($q_1 = 0$ deg, $q_2 = -90$ deg, $q_3 = 0$ deg, $q_4 = 90$ deg, $q_5 = 0$ deg, $q_6 = -90$ deg, $q_7 = 90$ deg; $l_0 = 0.2$ m, $l_1 = 0.115$ m, $l_2 = 0.115$ m, $l_3 = 0.135$ m, $l_4 = 0.261$ m, $l_5 = 0.239$ m, $l_6 = 0.3$ m, $l_7 = 0.1$ m)

$rank(^1M_4) = 2$. This case shows the necessity of the assumption (a) to assure the results of "**Theorem a.**"

5.2.2 The Nonsingular Configuration Assumption. "**Theorem a**" is to include realistic situation into the assumptions as (b_i), here we want to make the assumptions ideal for guaranteeing higher reconfiguration manipulability.

THEOREM b. *Let i be arbitrarily fixed such that $1 \leq i \leq n - 1$. Giving the nonsingular configuration assumption as*
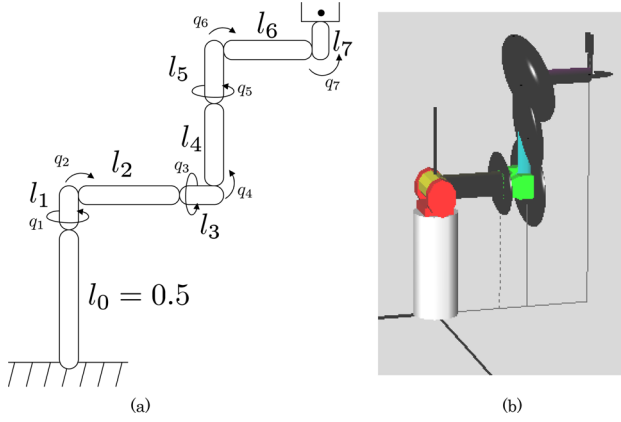
Fig. 16 Shape 12 of PA11 and reconfiguration manipulability ellipsoids ($q_1 = 0$ deg, $q_2 = -90$ deg, $q_3 = 0$ deg, $q_4 = 90$ deg, $q_5 = 0$ deg, $q_6 = -90$ deg, $q_7 = 90$ deg; $l_0 = 0.5$ m, $l_1 = 0.115$ m, $l_2 = 0.315$ m, $l_3 = 0.135$ m, $l_4 = 0.261$ m, $l_5 = 0.239$ m, $l_6 = 0.3$ m, $l_7 = 0.1$ m)
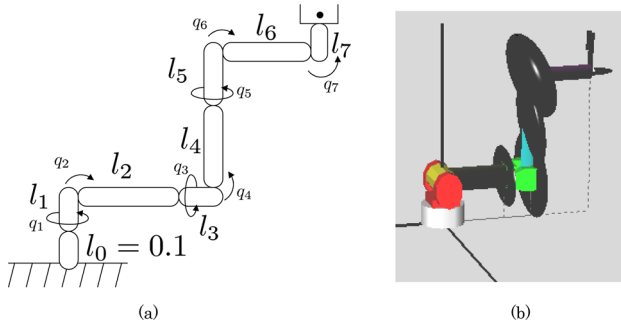
Fig. 17 Shape 13 of PA11 and reconfiguration manipulability ellipsoids ($q_1 = 0$ deg, $q_2 = -90$ deg, $q_3 = 0$ deg, $q_4 = 90$ deg, $q_5 = 0$ deg, $q_6 = -90$ deg, $q_7 = 90$ deg; $l_0 = 0.1$ m, $l_1 = 0.115$ m, $l_2 = 0.315$ m, $l_3 = 0.135$ m, $l_4 = 0.261$ m, $l_5 = 0.239$ m, $l_6 = 0.3$ m, $l_7 = 0.1$ m)

$$\begin{cases} (a). \ rank(\boldsymbol{J}_n^{n-m+1\to n}) = m \\ (b_i). \ rank(\boldsymbol{J}_i) = \min\{i, m\} \end{cases} \tag{56}$$

Then according to "**Theorem a**", *if* $n \geq 2m$

$$rank(^1\boldsymbol{M}_i) = \begin{cases} i(1 \leq i < m) \\ m(m \leq i \leq n - m) \\ n - i \sim m(n - m < i \leq n - 1) \end{cases} \tag{57}$$

If $m < n < 2m$

$$rank(^1\boldsymbol{M}_i) = \begin{cases} i(1 \leq i < n - m) \\ n - m(n - m \leq i \leq m) \\ n - i \sim n - m(m < i \leq n - 1) \end{cases} \tag{58}$$

Here, please note that the above assumption just declares $rank(\boldsymbol{J}_n^{n-m+1\to n})$ and $rank(\boldsymbol{J}_i)$, which indicates the $rank(J_p)(p \neq i)$ does not explicitly relate to $rank(^1\boldsymbol{M}_i)$. Along to this consideration, we name the second assumption as (b_i), which only concerns directly with kinematics from the base link to the ith link as shown in Fig. 19(a).

5.2.3 The Full-Nonsingular Configuration Assumption. Following the previous assumption in "**Theorem b**," we want to
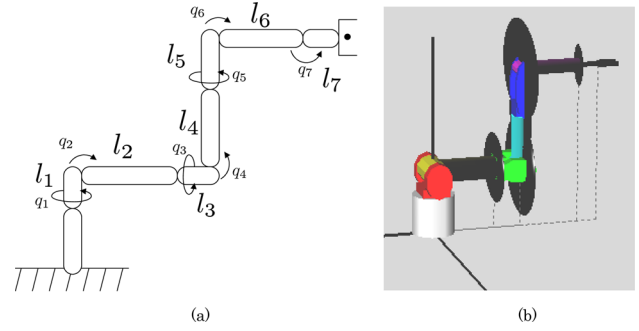
Fig. 18 Shape 14 of PA11 and reconfiguration manipulability ellipsoids ($q_1 = 0$ deg, $q_2 = -90$ deg, $q_3 = 0$ deg, $q_4 = 90$ deg, $q_5 = 0$ deg, $q_6 = -90$ deg, $q_7 = 0$ deg; $l_0 = 0.2$ m, $l_1 = 0.115$ m, $l_2 = 0.315$ m, $l_3 = 0.135$ m, $l_4 = 0.261$ m, $l_5 = 0.239$ m, $l_6 = 0.3$ m, $l_7 = 0.1$ m)
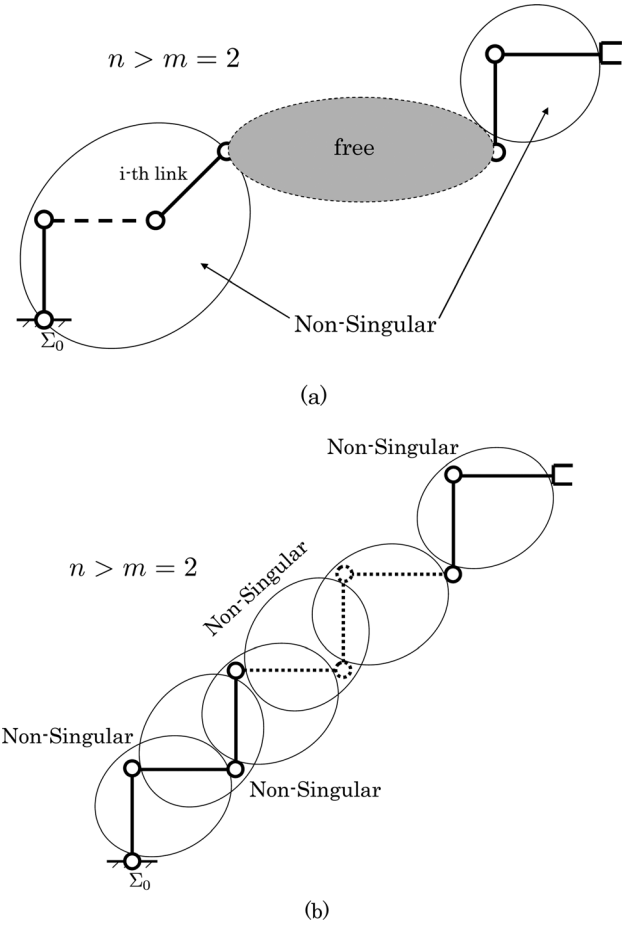
Fig. 19 Structure descriptions of two assumptions in two-dimensional space

pursue further full ideal assumptions to enlarge the reconfiguration manipulability to be maximum.

THEOREM c. *Given the full-nonsingular configuration assumption as*

$$rank(\boldsymbol{J}_i^{\nu\to\nu+m-1}) = \min\{i, m\}, \tag{59}$$
(all i satisfying $1 \leq i \leq n$; $\nu = \max\{i - m + 1, 1\}$)

the results Eqs. (57) and (58) are guaranteed.
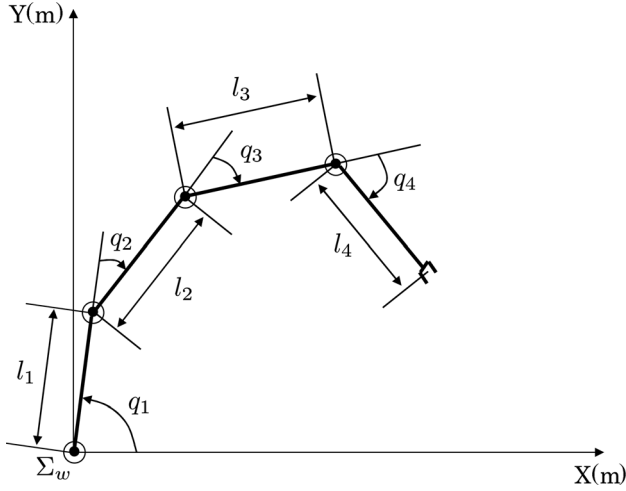
Fig. 20   4-link manipulator in two-dimensional space

Fig. 21   Manipulability ellipsoids

This means all possible partial configuration constituted by successive m links should be non-singular. The structure description of "Full-Nonsingular Configuration Assumption" is shown in Fig. 19(b). Because Eq. (59) includes Eq. (56), the results Eqs. (57) and (58) can be guaranteed.

Both the "Nonsingular Configuration Assumption" and "Full-Non-Singular Configuration Assumption" can guarantee Eqs. (57) and (58) from mathematical viewpoint. If we compare them from robotic viewpoint, on the one hand, the former is lower than the latter in the consideration of restriction degree of assumptions themselves. On the other hand, the former is wider than the latter in the consideration of their availability. However given multiple reconfiguration subtasks, the configuration complying full-nonsingular configuration assumption can keep higher reconfiguration manipulability for multiple reconfiguration subtasks since "Nonsingular Configuration Assumption" allows singular configuration in the "free area" of intermediate links depicted in Fig. 19(a), which reduces reconfiguration ability for further subtasks.

5.3   Judgment of Stoppage Possibility. For intermediate links, the simplest reconfiguration behavior is stop. This stopping-avoiding strategy will be exemplified in Sec. 6.2 with 7-link manipulator as shown in Fig. 26.

COROLLARY a. *Assuming the first reconfiguration subtask $^{1}\dot{r}_{id}$ in Eq. (8) is given as $^{1}\dot{r}_{id} = 0$, that is $\Delta^{1}\dot{r}_{id} = -J_i J_n^{+}\dot{r}_{nd}$. Then for all $\dot{r}_{nd} \in R^m$, admits $^{1}l \in R^n$ such that $\Delta^{1}\dot{r}_{id} = {}^{1}M_i^{1}l$ if and only if*

$$J_i J_n^{+} = {}^{1}M_i {}^{1}M_i^{+} J_i J_n^{+} \tag{60}$$

If we consider the case of $n - m < i \leq n$, the number of remaining links, i.e., from $(n - m + 1)$th link to nth link, is $m - 1$ and the dimensional number being realized by remaining links is less than m. Then, the realizable DoF of the remaining links becomes insufficient to keep the desired end-effector trajectory $\dot{r}_{nd}$ in m-dimensional space. So, discussing the stopping possibility of links within $n - m < i \leq n$ is out of the extent of prerequisite condition of arbitrarily given end-effector trajectory r_{nd} and $\dot{r}_{nd}$. Hence, here we think that the intermediate links satisfying $1 \leq i \leq n - m$ are possible to be stopped. Referring to the example of Fig. 26, we can find that only the links, the 1st to the 5th, can be stopped when the task of the end-effector has been given primarily. This result is consistent with "**Corollary a,**" only when $1 \leq i \leq 5$, Eq. (60) holds.

COROLLARY b. *As for redundant manipulator, assuming "Non-Singular Configuration Assumption" or "Full-Nonsingular Configuration Assumption" for all i satisfying $1 \leq i \leq n - m$. Then*
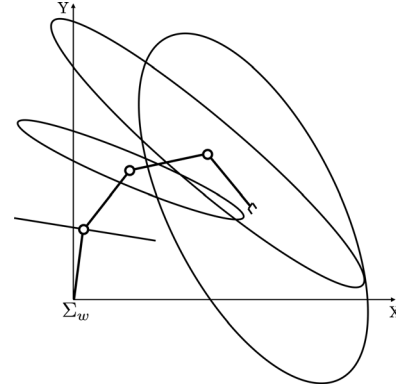
the intermediate links satisfying $1 \leq i \leq n - m$ can be stopped as the simplest reconfiguration behavior while the end-effector of the manipulator tracks the desired trajectory.

6   Examples

6.1   A Comparison of Manipulability Ellipsoid and Reconfiguration Manipulability Ellipsoid. Taking a 4-link redundant manipulator $(n = 4)$ in two-dimensional space $(m = m_p = 2)$ for example shown in Fig. 20. The definition of the kinematics of the manipulators used in this section follows the example shown in page 250 of Ref. [29] written by Yoshikawa. The origin of the working coordinate system Σ_w is fixed at the root of the first link. The joint angles, q_i ($i = 1, 2, 3, 4$ and unit is deg), are denoted along each rotational axis as counterclockwise direction is positive. All links are 0.25 in length ($i = 1, 2, 3, 4$, and unit is m).

To realize the given position of the end-effector at $r_{4d} = (0.6, 0.3)$, the joint angles are chosen to be $q_1 = 80$ deg, $q_2 = -30$ deg, $q_3 = -36$ deg, and $q_4 = -66$ deg, respectively, as a possible choice. In this given configuration, the manipulability ellipsoids and the reconfiguration manipulability ellipsoids are shown in Figs. 21 and 22, respectively. From Fig. 21, we can find that the size of manipulability ellipsoids becomes bigger and bigger as the link order increases. However, from Fig. 22, the reconfiguration manipulability ellipsoids corresponding to the first and the third links ($^{1P}P_1$ and $^{1P}P_3$) are denoted by two segments, which are partial reconfiguration manipulability ellipsoids represented by Eq. (15), meaning the first link and the third link can generate reconfiguration velocity along only one direction being vertical with the first link and the fourth link, respectively. The reconfiguration manipulability ellipsoid corresponding to the second link ($^{1C}P_2$) is complete reconfiguration manipulability ellipsoids denoted in Eq. (13) on the condition of $rank(^{1}M_2) = 2$. From the shape of reconfiguration manipulability ellipsoid $^{1C}P_2$, the longer main axis of $^{1C}P_2$ means the direction along which the second link can generate the highest reconfiguration velocity, the shorter main axis of $^{1C}P_2$ means the direction along which the link generates the smallest velocity.

From Fig. 22, we can find that the size of the reconfiguration manipulability ellipsoids spreads from the manipulator's base, also spreading reversely from the end-effector to the base, which results in an improved reconfiguration manipulability for joints which are more or less the middle of the kinematic chain. The redundant manipulator in the plane will always have degenerated ellipsoids $^{1P}P_1$ and $^{1P}P_{n-1}$. Moreover, by comparing Fig. 21 with Fig. 22, it is clear that the size of each avoidance manipulability ellipsoid in Fig. 21 is smaller than the corresponding size of manipulability ellipsoid in Fig. 22 because the singular values of $^{1}M_i$ are smaller than the ones of J_i.

If the end-effector of the manipulator r_{4d} is designated at three different positions on the x-axis, as (0.3, 0.0), (0.6, 0.0), and (0.9, 0.0). The initial configuration of manipulator is that
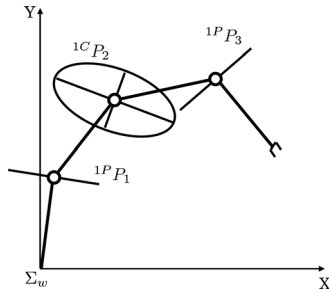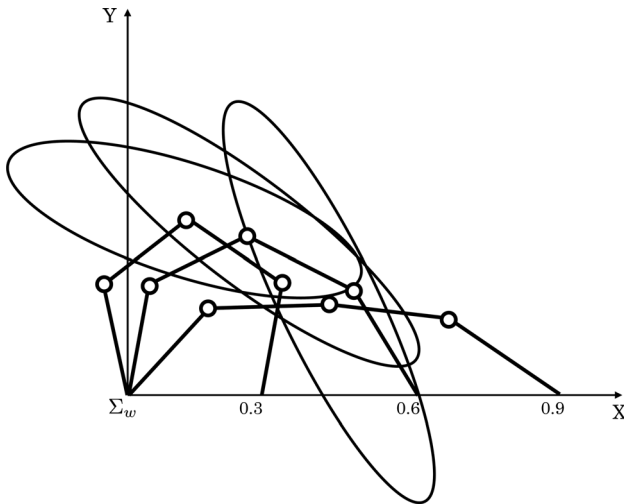
Fig. 22 Reconfiguration manipulability ellipsoids

Fig. 24 Reconfiguration manipulability ellipsoid of the second link

Fig. 23 Manipulability ellipsoid of the second link

Fig. 25 Manipulability measure/reconfiguration manipulability measure

$q_1 = 100$ deg, $q_2 = -60$ deg, $q_3 = -80$ deg, and $q_4 = -60$ deg. Figures 23 and 24 show the manipulability ellipsoids and the reconfiguration manipulability ellipsoids of the second link when the end-effector of the manipulator is fixed at these three different positions, respectively. By comparing Fig. 23 with Fig. 24, we can see that the size of manipulability ellipsoid does not change so much, adversely, the size of reconfiguration manipulability ellipsoid changes remarkably. We evaluate the manipulability measure and the reconfiguration manipulability measure by the sum of their ellipsoid areas. Figure 25 shows the changes of manipulability measure S_{M2} in Eq. (4) and reconfiguration manipulability measure S_{RM2} in Eq. (18) of the second link, while the end-effector of the manipulator changes from (0.0, 0.0) to (1.0, 0.0) in *x*-axis. Please note that manipulability measure and reconfiguration manipulability measure are evaluated by the area of manipulability ellipsoid and reconfiguration manipulability ellipsoid. From Fig. 25, we find that the second link can keep the high manipulability measure in the whole moving extent. However, the reconfiguration manipulability measure of the second link decreases quickly as the end-effector of the manipulator is far away the root of the first link, which indicates that it is better to make the end-effector of the manipulator do something such as trajectory tracking or obstacle avoidance near the root of the first link for keep higher reconfiguration manipulability.

6.2 Stoppage of Intermediate Links. Figures 26 and 27 show the change processes of the reconfiguration manipulability ellipsoids when a 7-link manipulator tracks the desired trajectory and avoids a circular obstacle in two-dimensional space. The initial configuration is that $q_1 = 90$ deg, $q_2 = -30$ deg, $q_3 = -30$ deg, $q_4 = -30$ deg, $q_5 = -30$ deg, and $q_6 = -30$ deg and $q_7 = -30$ deg, where this initial configuration satisfies "Full-Non-Singular Configuration Assumption" given by
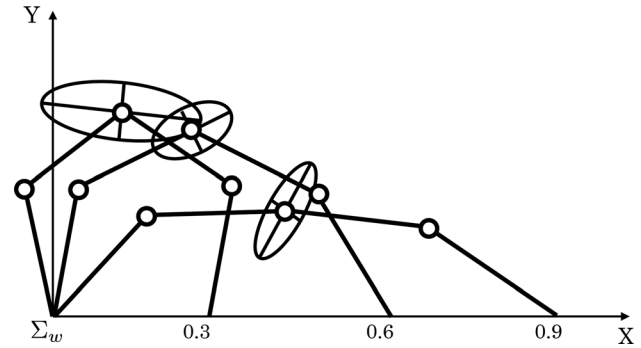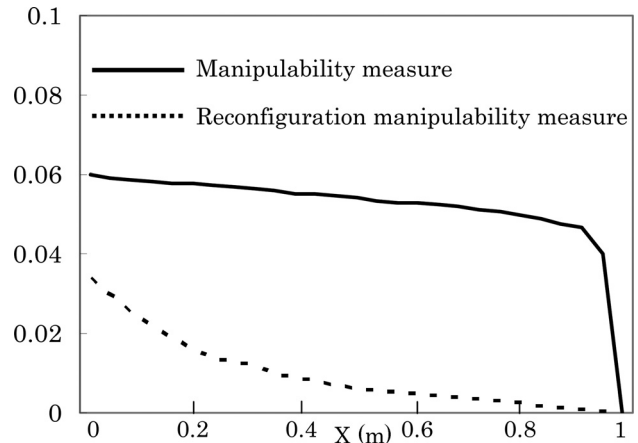
Eq. (59). All links are 0.2 in length ($i = 1, \ldots, 7$). The shape of obstacle is a circle with radius of $r = 0.19$ m shown in Fig. 26, the center of obstacle is fixed at (0.25, 0.10). In Fig. 27, the center of obstacle is fixed at (0.31, 0.25). In the process of trajectory tracking of the end-effector, the *i*th link will be stopped (the demanded reconfiguration velocity is zero discussed in Sec. 5.3) for avoiding the collision with the obstacle once the distance between the tip of the *i*th link r_i and the center of the obstacle is less than 1.25 r.

From Fig. 26, in the process of trajectory tracking and obstacle avoidance, the tip of the first link is stopped when it nears the obstacle, that is to say, the first demanded reconfiguration velocity ${}^1\dot{\boldsymbol{r}}_{d1} = 0$ is realized (the first reconfiguration subtask is finished). Then, the size of the second reconfiguration manipulability ellipsoids changes after finishing the first reconfiguration subtask. The second reconfiguration manipulability ellipsoid of the second link becomes a segment, and the others become smaller. In this way, the manipulator can execute the second (${}^2\dot{\boldsymbol{r}}_{d2} = 0$), third (${}^3\dot{\boldsymbol{r}}_{d3} = 0$), fourth (${}^4\dot{\boldsymbol{r}}_{d4} = 0$), and fifth demanded reconfiguration subtasks (${}^5\dot{\boldsymbol{r}}_{d5} = 0$) in sequence. The changed reconfiguration manipulability ellipsoids become segment or smaller after finishing the current reconfiguration subtask. Finally, the manipulator finishes the desired trajectory tracking and obstacle avoidance, however, the reconfiguration ability of whole manipulator disappears and it cannot continue to track trajectory and avoid obstacle simultaneously after these five demanded reconfiguration subtasks have been realized because redundancy has disappeared. This specific example in Fig. 26 just verifies "**Corollary b**".

In Fig. 27, in the process of trajectory tracking and obstacle avoidance, the first reconfiguration subtask (${}^1\dot{\boldsymbol{r}}_{d3} = 0$) is given to the tip of the third link. After finishing this first reconfiguration subtask, the second reconfiguration manipulability ellipsoids
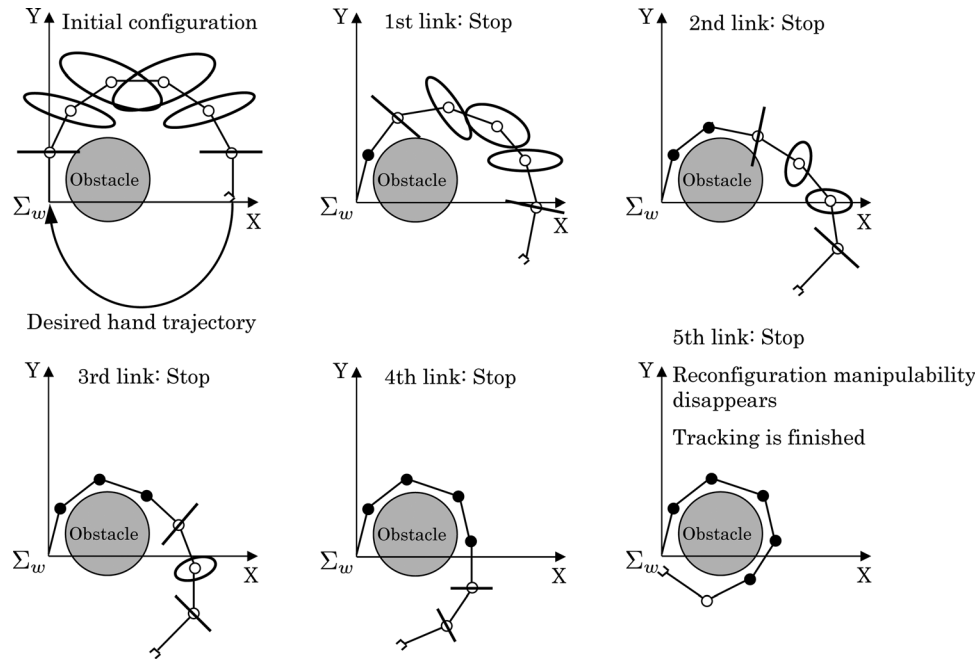
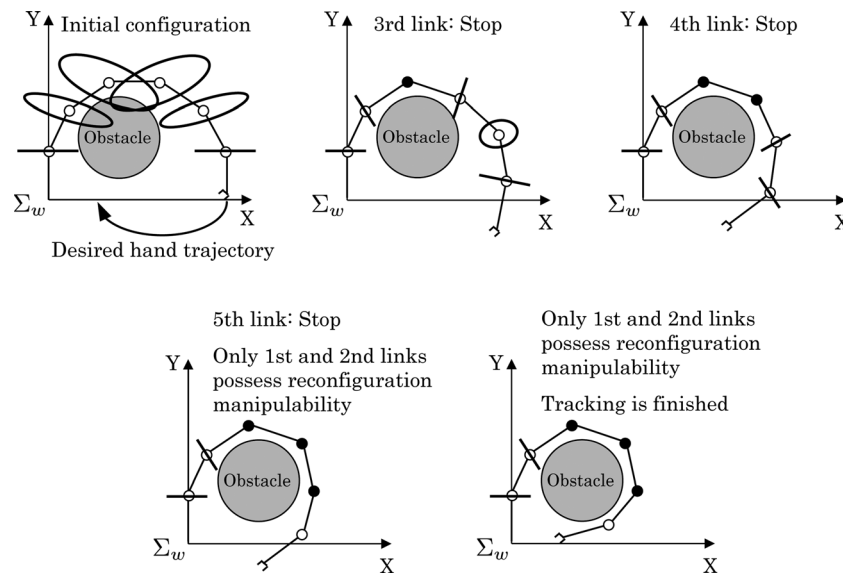**Fig. 26   Stoppage operation process 1**

Fig. 27   Stoppage operation process 2

become smaller, especially, the second reconfiguration manipulability ellipsoids of the second and fourth links become segments. Then, the second and third reconfiguration subtasks are given to the fourth and fifth links respectively, that is, $^2\dot{\boldsymbol{r}}_{d4} = 0$ and $^3\dot{\boldsymbol{r}}_{d5} = 0$. Finally, the manipulator finishes the desired trajectory tracking and obstacle avoidance, it cannot continue to track trajectory and avoid obstacle simultaneously after these three reconfiguration subtasks are finished. However, the first and second links still possess the reconfiguration ability in Fig. 27. This is the difference between Figs. 26 and 27. These results are consistent with "**Corollary a**" and "**Corollary b**".

7   Discussion

Here, we will conceptually introduce the reconfiguration manipulability into the application of humanoid robot as an example. As shown in Fig. 28, there is a humanoid robot with visual servoing system. The whole body of this humanoid robot, from the foots to the head, can be described by a redundant manipulator. The foots touch the ground and are fixed at the base coordinate. The head may be thought to represent the end-effector of the redundant manipulator. Especially, the robot's eyes are used as visual servoing system by installing a camera or several ones. Humanoid robot mainly has two kinds of tasks. On the one hand, visual servoing system is used for executing the prior end-effector task, by which the camera can on-line track some moving target to keep its head's pose as required. On the other hand, some appropriate shape-adjustments of the body by controlling the motion of the intermediate links for keeping the stability of humanoid robot are thought to be reconfiguration subtasks.

According to above discussion, the possibility of stabilizing control as the secondary subtasks can be described in the
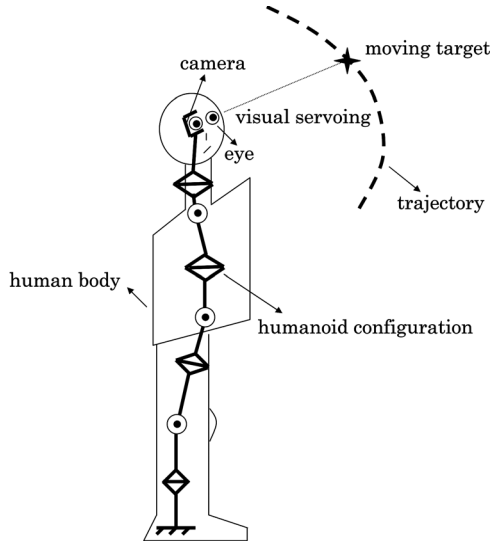
Fig. 28 Humanoid robot with visual servoing system

reconfiguration space and restricted strictly in the range space of ^1M_i, which is the main result of this research. Therefore, based on the sufficient conditions to keep the expansion of the reconfiguration space, the dimension of the stabilizing motion of the humanoid robot can be maintained by "Non-Singular Configuration Assumption" or "Full-Non-Singular Configuration Assumption," since it guarantees the sustainability of stabilizing motion.

8 Conclusion

In this paper, we proposed reconfiguration manipulability concept to measure shape-changeability of the intermediate links providing a prior end-effector task is given. Through analyses of multiple reconfiguration matrices, whether multiple reconfiguration subtasks can be executed or not, and how many subtasks are realizable can be judged on-line. Furthermore, the sufficient conditions have been shown that they can prove mathematically the sustainability of the reconfiguration space of intermediate links by nonsingular decomposition analyses of reconfiguration matrix. Further, we confirmed the proposed analyses can be useful practically for evaluating the realistic manipulator's configurations and structures.

Besides being applied in obstacle avoidance of redundant manipulator discussed in this research as a basic example, reconfiguration manipulability can be used to analyze the realizability of body balancing motion of the humanoid robot as a subtask with prior head motion. Therefore, we think that the proposal of reconfiguration manipulability can lay fundamental base for a particular research direction for redundant robot. ts and suggestions on this paper.

Appendix

Proofs. *Proof of Proposition a.*

$$^1M_n = 0 \tag{A1}$$

"**Proposition a**" follows.
Proof of Proposition b.
According to Eqs. (2), (36) and (42), ^1M_i can be decomposed as

$$^1M_i = \tilde{J}_i V_{i,(n-m)} \, V_{n-m}^T \tag{A2}$$

then, we can obtain

$$rank(^1M_i) \geq rank(\tilde{J}_i) + rank(V_{i,(n-m)}) - i \tag{A3}$$

and

$$rank(^1M_i) \leq \min\{rank(\tilde{J}_i), rank(V_{i,(n-m)}), n-m\} \tag{A4}$$

In Eqs. (A3) and (A4), we use an important mathematical theory: assuming A is $n \times m$ matrix and B is $m \times l$ matrix, then

$$rank(A) + rank(B) - m \leq rank(AB) \leq \min\{rank(A), rank(B)\} \tag{A5}$$

"**Proposition b**" follows.
Proof of Lemma a. Because $rank(J_n^{n-m+1 \to n}) = m$, we can obtain $rank(J_n) = m$, so, referring to Eq. (29), J_n can be decomposed by

$$\begin{aligned} J_n &= U_m \Sigma_m V_m^T \\ &= R_m V_m^T \end{aligned} \tag{A6}$$

In Eq. (A6), because $rank(U_m) = m$ and $rank(\Sigma_m) = m$, $rank(R_m) = rank(U_m \Sigma_m) = m$. Then, according to Eq. (A6), we can obtain

$$V_m^T = R_m^{-1} J_n \tag{A7}$$

above equation can be rewritten as

$$[V_{(n-m),m}^T, V_{m,m}^T] = R_m^{-1} J_n \tag{A8}$$

According to Eq. (A8) and the definition of $J_n^{n-m+1 \to n}$, we can obtain

$$V_{m,m}^T = R_m^{-1} J_n^{n-m+1 \to n} \tag{A9}$$

In above equation, because $rank(R_m^{-1}) = m$ and $rank(J_n^{n-m+1 \to n}) = m$, we can obtain

$$\begin{aligned} rank(V_{m,m}^T) &= rank(V_{m,m}) \\ &= m \end{aligned} \tag{A10}$$

In addition, from Eq. (39), V can be simply expressed as

$$V = \begin{bmatrix} A & C \\ B & D \end{bmatrix} \tag{A11}$$

then, we can obtain that

$$V^T V = \begin{bmatrix} A^T A + B^T B & A^T C + B^T D \\ C^T A + D^T B & C^T C + D^T D \end{bmatrix} \tag{A12}$$

and

$$V V^T = \begin{bmatrix} A A^T + C C^T & A B^T + C D^T \\ B A^T + D C^T & B B^T + D D^T \end{bmatrix} \tag{A13}$$

And because of the condition that

$$V^T V = I_n \tag{A14}$$

then, from Eq. (A12), we can obtain

$$A^T A + B^T B = I_m \tag{A15}$$

Because of the condition that

$$VV^T = I_n \tag{A16}$$

then, from Eq. (A13), we can obtain

$$AA^T + CC^T = I_{n-m} \tag{A17}$$

A^T and A can be expressed by singular value decomposition as

$$A^T = {}^A U {}^A \Sigma {}^A V^T \tag{A18}$$

and

$$A = {}^A V {}^A \Sigma^{TA} U^T \tag{A19}$$

In Eqs. (A18) and (A19), ${}^A U$ is $m \times m$ matrix satisfying ${}^A U {}^A U^T = {}^A U^T {}^A U = I_m$, ${}^A \Sigma$ is $m \times (n - m)$ matrix including singular values of A, ${}^A V$ is $(n - m) \times (n - m)$ matrix satisfying ${}^A V {}^A V^T = {}^A V^T {}^A V = I_{n-m}$. Then, we can obtain

$$A^T A = {}^A U {}^A \Sigma {}^A \Sigma^{TA} U^T \tag{A20}$$

and

$$AA^T = {}^A V {}^A \Sigma^{TA} \Sigma {}^A V^T \tag{A21}$$

According to Eqs. (A17) and (A20), we can obtain

$$B^T B = {}^A U (I_m - {}^A \Sigma {}^A \Sigma^T) {}^A U^T \tag{A22}$$

then, we can obtain

$$I_m - {}^A \Sigma {}^A \Sigma^T = {}^A U^T B^T B {}^A U \tag{A23}$$

In Eq. (A23), because $rank(B) = m$ and $rank({}^A U) = m$ (here, please note that B and ${}^A U$ are $m \times m$ matrices), so we can obtain

$$rank(I_m - {}^A \Sigma {}^A \Sigma^T) = m \tag{A24}$$

If $n \geq 2m$, according to Eqs. (A17) and (A21), we can obtain

$$CC^T = {}^A V \begin{bmatrix} I_m - {}^A \Sigma {}^A \Sigma^T & \varnothing \\ \varnothing & I_{n-2m} \end{bmatrix} {}^A V^T \tag{A25}$$

In Eq. (A25), because of Eq. (A24), we can obtain

$$rank\left(\begin{bmatrix} I_m - {}^A \Sigma {}^A \Sigma^T & \varnothing \\ \varnothing & I_{n-2m} \end{bmatrix} \right) = n - m \tag{A26}$$

and because $rank({}^A V) = n - m$ and Eq. (A26), we can obtain $rank(CC^T) = n - m$, that is, $rank(C) = n - m$.

On the other hand, if $m < n < 2m$, according to Eqs. (A17) and (A21), we can obtain

$$CC^T = {}^A V (I_{n-m} - {}^A \Sigma^{TA} \Sigma) {}^A V^T \tag{A27}$$

In above equation, because $n - m < m$, we can obtain the relation as

$$I_m - {}^A \Sigma {}^A \Sigma^T = \begin{bmatrix} I_{n-m} - {}^A \Sigma^{TA} \Sigma & \varnothing \\ \varnothing & I_{2m-n} \end{bmatrix} \tag{A28}$$

Because $rank(I_m - {}^A \Sigma {}^A \Sigma^T) = m$ in Eq. (A24) and $rank(I_{2m-n}) = 2m - n$, we can obtain

$$rank(I_{n-m} - {}^A \Sigma^{TA} \Sigma) = m - (2m - n) = n - m \tag{A29}$$

and because $rank({}^A V) = n - m$ and Eq. (A27), we can obtain $rank(CC^T) = n - m$, that is, $rank(C) = n - m$.

According to above discussion, in the two conditions of $n \geq 2m$ and $m < n < 2m$, we can obtain (here, please note $C = V_{(n-m),(n-m)}$ in Eq. (39))

$$rank(V_{(n-m),(n-m)}) = n - m \tag{A30}$$

Then, when $1 \leq i < n - m$, we can obtain the relation between $V_{i,(n-m)}$ and $V_{(n-m),(n-m)}$ as

$$V_{(n-m),(n-m)} = \begin{bmatrix} V_{i,(n-m)} \\ V_{(n-m-i),(n-m)} \end{bmatrix} \tag{A31}$$

According to Eqs. (A30) and (A31), $V_{(n-m),(n-m)}$ is $(n - m) \times (n - m)$ matrix with full rank. Since $V_{i,(n-m)}$ is $i \times (n - m)$ matrix and $V_{i,(n-m)}$ is one part of $V_{(n-m),(n-m)}$, then the jth $(j = 1, \ldots, i)$ row vectors of $V_{i,(n-m)}$ are independent and we can obtain $rank(V_{i,(n-m)}) = i$.

When $n - m \leq i \leq n$, we can obtain the relation between $V_{i,(n-m)}$ and $V_{(n-m),(n-m)}$ as

$$V_{i,(n-m)} = \begin{bmatrix} V_{(n-m),(n-m)} \\ V_{(i-n+m),(n-m)} \end{bmatrix} \tag{A32}$$

According to Eqs. (A30) and (A32), $V_{(n-m),(n-m)}$ is one part of $V_{i,(n-m)}$, then the jth $(j = 1, \ldots, n - m)$ column vectors of $V_{i,(n-m)}$ are independent and we can obtain $rank(V_{i,(n-m)}) = n - m$. In this way, we can obtain

$$rank(V_{i,(n-m)}) = \begin{cases} i & 1 \leq i < n - m \\ n - m & n - m \leq i \leq n \end{cases} \tag{A33}$$

"**Lemma a**" follows.

Proof of Theorem a. According to Eqs. (2), (45), and (48), "**Theorem a**" follows.

Proof of Theorem b. If $\{n \geq 2m\} \cap \{1 \leq i < m\}$ or $\{m < n < 2m\} \cap \{1 \leq i < n - m\}$, we know that $i < m \leq n - m$ or $i < n - m < m$, by inputting these conditions into "**Theorem a**" Eq. (50), we can obtain

$$rank({}^1 M_i) = i \tag{A34}$$

If $\{n \geq 2m\} \cap \{m \leq i \leq n - m\}$, we know that $m \leq i \leq n - m$, by inputting this condition into "**Theorem a**" Eq. (50), we can obtain

$$rank({}^1 M_i) = m \tag{A35}$$

If $\{m < n < 2m\} \cap \{n - m \leq i \leq m\}$, we know that $n - m \leq i \leq m$, by inputting this condition into "**Theorem a**" Eq. (50), we can obtain

$$rank({}^1 M_i) = n - m \tag{A36}$$

If $\{n \geq 2m\} \cap \{n - m < i \leq n - 1\}$, we know that $m \leq n - m < i$, by inputting this condition into "**Theorem a**" Eq. (50), we can obtain

$$n - i \leq rank({}^1 M_i) \leq m \tag{A37}$$

If $\{m < n < 2m\} \cap \{m < i \leq n - 1\}$, we know that $n - m < m < i$, by inputting this condition into "**Theorem a**" Eq. (50), we can obtain

$$n - i \leq rank(^1\boldsymbol{M}_i) \leq n - m \tag{A38}$$

In this way, "**Theorem b**," Eqs. (57) and (58) are proved in above five conditions as shown Eqs. (A34)–(A38).

Proof of Theorem c. In Eq. (59), when $i = n$ and $\nu = n - m + 1$, we can obtain

$$\begin{aligned}
rank(\boldsymbol{J}_i^{\nu \to \nu + m - 1}) &= rank(\boldsymbol{J}_n^{n - m + 1 \to n}) \\
&= \min\{n, m\} \\
&= m
\end{aligned} \tag{A39}$$

which corresponds to (a) of Eq. (56). By Eq. (A39), we finish the proof that "Full-Non-Singular Configuration Assumption" includes "Nonsingular Configuration Assumption (a)".

From Eq. (59), when $i < m$ and $\nu = 1$, we can obtain

$$\begin{aligned}
rank(\boldsymbol{J}_i^{\nu \to \nu + m - 1}) &= rank(\boldsymbol{J}_i^{1 \to m}) \\
&= rank(\tilde{\boldsymbol{J}}_i) \\
&= i,
\end{aligned} \tag{A40}$$

when $m < i$ and $\nu = i - m + 1$, we can obtain

$$\begin{aligned}
rank(\boldsymbol{J}_i^{\nu \to \nu + m - 1}) &= rank(\boldsymbol{J}_i^{i - m + 1 \to i}) \\
&= m
\end{aligned} \tag{A41}$$

then, we can obtain

$$rank(\tilde{\boldsymbol{J}}_i) = m \tag{A42}$$

Then, Eqs. (A40) and (A42) can be combined as

$$rank(\tilde{\boldsymbol{J}}_i) = \min\{i, m\} \tag{A43}$$

that is

$$rank(\boldsymbol{J}_i) = \min\{i, m\} \tag{A44}$$

which is identical to "nonsingular configuration assumption (b_i)" of "**Theorem a**". In this way, we finish the proof that "Full-Non-Singular Configuration Assumption" includes "Nonsingular configuration assumption (b_i)."

Proof of Corollary a. Put $\Delta^1 \dot{\boldsymbol{r}}_{\text{id}} = -\boldsymbol{J}_i \boldsymbol{J}_n^+ \dot{\boldsymbol{r}}_{\text{nd}}$. There exists $^1\boldsymbol{l} \in R^n$ such that $\Delta^1 \dot{\boldsymbol{r}}_{\text{id}} = {}^1\boldsymbol{M}_i^1 \boldsymbol{l}$ if and only if $\Delta^1 \dot{\boldsymbol{r}}_{\text{id}} \in R(^1\boldsymbol{M}_i)$. That is $\Delta^1 \dot{\boldsymbol{r}}_{\text{id}} = {}^1\boldsymbol{M}_i^1 \boldsymbol{M}_i^+ \Delta^1 \dot{\boldsymbol{r}}_{\text{id}}$, which is equivalent to $\boldsymbol{J}_i \boldsymbol{J}_n^+ \dot{\boldsymbol{r}}_{\text{nd}} = {}^1\boldsymbol{M}_i^1 \boldsymbol{M}_i^+ \boldsymbol{J}_i \boldsymbol{J}_n^+ \dot{\boldsymbol{r}}_{\text{nd}}$. Since $\dot{\boldsymbol{r}}_{\text{nd}}$ has been assumed to be given arbitrarily in m-dimension, it follows $\boldsymbol{J}_i \boldsymbol{J}_n^+ = {}^1\boldsymbol{M}_i^1 \boldsymbol{M}_i^+ \boldsymbol{J}_i \boldsymbol{J}_n^+$.

Proof of Corollary b. In "Nonsingular Configuration Assumption" or "Full-Nonsingular Configuration Assumption" for all i satisfying $1 \leq i \leq n - m$. From "**Theorem a**," when $1 \leq i \leq n - m$, we can obtain $rank(\boldsymbol{J}_i) = rank(^1\boldsymbol{M}_i) = \min\{i, m\}$. In addition, $\boldsymbol{J}_i$ and $^1\boldsymbol{M}_i$ can be decomposed as $\boldsymbol{J}_i = \boldsymbol{B}'\boldsymbol{C}'$ and $^1\boldsymbol{M}_i = \boldsymbol{B}'\boldsymbol{D}'$. $\boldsymbol{B}'$ is $m \times i$ matrix, $\boldsymbol{C}'$ and $\boldsymbol{D}'$ are $i \times n$ matrices. Referring to Eqs. (2) and (44), $\boldsymbol{B}', \boldsymbol{C}',$ and $\boldsymbol{D}'$ can be described as

$$\begin{cases}
\boldsymbol{B}' = \tilde{\boldsymbol{J}}_i \\
\boldsymbol{C}' = (\boldsymbol{I}_i \boldsymbol{0}) \\
\boldsymbol{D}' = \boldsymbol{V}_{i,(n-m)} \boldsymbol{V}_{n-m}^T
\end{cases} \tag{A45}$$

and it is easy to know

$$\begin{cases}
rank(\boldsymbol{B}') = \min\{i, m\} \\
rank(\boldsymbol{C}') = i
\end{cases} \tag{A46}$$

and

$$rank(\boldsymbol{D}') = \min\{i, n - m\} = i \tag{A47}$$

because $rank(\boldsymbol{V}_{i,(n-m)}) + rank(\boldsymbol{V}_{n-m}^T) - (n - m) \leq rank(\boldsymbol{D}') \leq \min\{rank(\boldsymbol{V}_{i,(n-m)}), rank(\boldsymbol{V}_{n-m}^T)\}$, that is $rank(\boldsymbol{V}_{i,(n-m)}) \leq rank(\boldsymbol{D}') \leq \min\{rank(\boldsymbol{V}_{i,(n-m)}), n - m\}$, that is $\min\{i, n - m\} \leq rank(\boldsymbol{D}') \leq \min\{\min\{i, n - m\}, n - m\}$, resulting in $rank(\boldsymbol{D}') = i$ in this case referring to Eq. (A33).

Then, if $\{1 \leq i < m \leq n - m\} \cup \{1 \leq i \leq n - m < m\}$, we can obtain

$$\begin{aligned}
{}^1\boldsymbol{M}_i^1 \boldsymbol{M}_i^+ \boldsymbol{J}_i \boldsymbol{J}_n^+ &= \boldsymbol{B}'\boldsymbol{D}'[\boldsymbol{D}'^T(\boldsymbol{D}'\boldsymbol{D}'^T)^{-1}(\boldsymbol{B}'^T\boldsymbol{B}')^{-1}\boldsymbol{B}'^T]\boldsymbol{B}'\boldsymbol{C}'\boldsymbol{J}_n^+ \\
&= \boldsymbol{B}'[\boldsymbol{D}'\boldsymbol{D}'^T(\boldsymbol{D}'\boldsymbol{D}'^T)^{-1}(\boldsymbol{B}'^T\boldsymbol{B}')^{-1}\boldsymbol{B}'^T\boldsymbol{B}']\boldsymbol{C}'\boldsymbol{J}_n^+ \\
&= \boldsymbol{B}'\boldsymbol{C}'\boldsymbol{J}_n^+ \\
&= \boldsymbol{J}_i \boldsymbol{J}_n^+
\end{aligned} \tag{A48}$$

If $m \leq i \leq n - m$, because $^1\boldsymbol{M}_i$ is row full rank matrix, that is $rank(^1\boldsymbol{M}_i) = m$, we can simply obtain

$$\begin{aligned}
{}^1\boldsymbol{M}_i^1 \boldsymbol{M}_i^+ \boldsymbol{J}_i \boldsymbol{J}_n^+ &= {}^1\boldsymbol{M}_i^1 \boldsymbol{M}_i^T(^1\boldsymbol{M}_i^1 \boldsymbol{M}_i^T)^{-1}\boldsymbol{J}_i \boldsymbol{J}_n^+ \\
&= \boldsymbol{J}_i \boldsymbol{J}_n^+
\end{aligned} \tag{A49}$$

References

[1] Yoshikawa, T., 1984, "Measure of Manipulability for Robot Manipulators," J. Rob. Soc. Jpn., **2**(1), pp. 63–71. (in Japanese).

[2] Yoshikawa, T., 1985, "Manipulability of Robot Mechanisms," Int. J. Robot. Res., **4**(2), pp. 3–9.

[3] Maciejewski, A. A., and Klein, C. A., 1985, "Obstacle Avoidance for Kinematically Redundant Manipulators in Dynamically Varying Environments," Int. J. Robot. Res., **4**(3), pp. 109–117.

[4] Nakamura, Y., Hanafusa, H., and Yoshikawa, T., 1987, "Task-Priority Based Redundancy Control of Robot Manipulators," Int. J. Robot. Res., **6**(2), pp. 3–15.

[5] Lee, S., 1989, "Dual Redundant Arm Configuration Optimization With Task-Oriented Dual Arm Manipulability," IEEE Trans. Rob. Autom., **5**(1), pp. 78–97.

[6] Chiacchio, P., Chiaverini, S., Sciavicco, L., and Siciliano, B., 1991, "Global Task Space Manipulability Ellipsoids for Multiple-Arm System," IEEE Trans. Rob. Autom., **7**(5), pp. 678–685.

[7] Huang, J., Yamada, D., Nakamura, Y., Hara, M., and Yabuta, T., 2009, "Cooperative Impedance Control of a Finger-Arm Robot by Regulating Finger's Manipulability," J. Syst. Des. Dyn., **3**(5), pp. 756–767.

[8] Bicchi, A., Melchiorri, C., and Balluchi, D., 1995, "On the Mobility and Manipulability of General Multiple Limb Robots," IEEE Trans. Rob. Autom., **11**(2), pp. 215–228.

[9] Kawasaki, H., and Mouri, T., 2007, "Design and Control of Five-Fingered Haptic Interface Opposite to Human Hand," IEEE Trans. Rob. Autom., **23**(5), pp. 909–918.

[10] Koeppe, R., and Yoshikawa, T., 1997, "Dynamic Manipulability Analysis of Compliant Motion," Proceedings of IEEE/RSJ International Conference on Intelligent Robots and Systems, Grenoble, Vol. 3, pp. 1472–1478.

[11] Yoshikawa, T., 1985, "Dynamic Manipulability of Robot Manipulators," IEEE Int. Conf. Rob. Autom., **2**, pp. 1033–1038.

[12] Chiacchio, P., 2000, "A New Dynamic Manipulability Ellipsoid for Redundant Manipulators," Robotica, **18**(4), pp. 381–387.

[13] Kurazume, R., and Hasegawa, T., 2002, "Impedance Matching for Free Flying Robots," Proceedings of the 20th Annuual Conference Robotics Society of Japan, Paper No. 3J16. (in Japanese).

[14] Kurazume, R., and Hasegawa, T., 2006, "A New Index of Serial-Link Manipulator Performance Combining Dynamic Manipulability and Manipulating Force Ellipsoid," IEEE Trans. Rob. Autom., **22**(5), pp. 1022–1028.

[15] Bowling, A., and Khatib, O., 2005, "The Dynamic Capability Equations: A New Tool for Analyzing Robotic Manipulator Performance," IEEE Trans. Rob. Autom., **21**(1), pp. 115–123.

[16] Shugen, M., and Watanabe, M., 2000, "Minimum Time Path-Tracking Control of Redundant Manipulators," International Conference on Intelligent Robots and Systems, Takamatsu, **1**, pp. 27–32.

[17] Jamisola, R. S. Jr., Maciejewski, A. A., and Roberts, R. G., 2006, "Failure-Tolerant Path Planning for Kinematically Redundant Manipulators Anticipating Locked-Joint Failures," IEEE Trans. Rob. Autom., **22**(4), pp. 603–612.

[18] Ahuactzin, J. M., and Gupta, K. K., 1999, "The Kinematic Roadmap: A Motion Planning Based Global Approach for Inverse Kinematics of Redundant Robots," IEEE Trans. Rob. Autom., **15**(4), pp. 653–669.

[19] Glass, K., Colbaugh, R., Lim, D., and Seraji, H., 1995, "Real-Time Collision Avoidance for Redundant Manipulators," IEEE Trans. Rob. Autom., **11**, pp. 448–457.

[20] Seraji, H., and Bon, B., 1999, "Real-Time Collision Avoidance for Position-Controlled Manipulators," IEEE Trans. Rob. Autom., **15**(4), pp. 670–677.

[21] Zlajpah, L., and Nemec, B., 2002, "Kinematic Control Algorithms for On-Line Obstacle Avoidance for Redundant Manipulator," International Conference on Intelligent Robots and Systems, Lausanne, Vol. 2, pp. 1898–1903.

[22] Lee, K.-K., and Buss, M., 2007, "Obstacle Avoidance for Redundant Robots Using Jacobian Transpose Method," International Conference on Intelligent Robots and Systems, San Diego, pp. 3509–3514.

[23] Marani, G., and Jinhyun, K., 2002, "A Real-Time Approach for Singularity Avoidance in Resolved Motion Rate Control of Robotic Manipulator," Proceedings of IEEE/RSJ International Conference on Robotics and Automation, Washington, Vol. 2, pp. 1973–1978.

[24] Minami, M., and Takahara, M., 2003, "Avoidance Manipulability for Redundant Manipulators," IEEE/ASME International Conference on Advanced Intelligent Mechatronics, No. 140, pp. 314–319.

[25] Siciliano, B., and Slotine, J. J. E., 1991, "A General Framework for Managing Multiple Tasks in Highly Redundant Robotic Systems," Fifth International Conference on Advanced Robotics, Vol. 2, pp. 1211–1216.

[26] Tanaka, H., Minami, M., and Mae, Y., 2005, "Trajectory Tracking of Redundant Manipulators Based on Avoidance Manipulability Shape Index," Proceedings of IEEE/RSJ International Conference on Intelligent Robots and Systems, Edmonton, pp. 1892–1897.

[27] Ikeda, K., Tanaka, H., Zhang, T., Minami, M., and Mae, Y., 2006, "On-line Optimization of Avoidance Ability for Redundant Manipulator," Proceedings of IEEE/RSJ International Conference on Intelligent Robots and Systems, Beijing, pp. 592–597.

[28] Zhang, T., Minami, M., and Song, W., 2007, "Multi-Preview Configuration Control for Redundant Manipulator by Future Reachability Evaluation," Proceedings of IEEE/RSJ International Conference on Intelligent Robots and Systems, SanDiego, pp. 3503–3508.

[29] Yoshikawa, T., 1990, *Foundations of Robotics: Analysis and Control*, MIT, MIT Press, Cambridge, MA.